

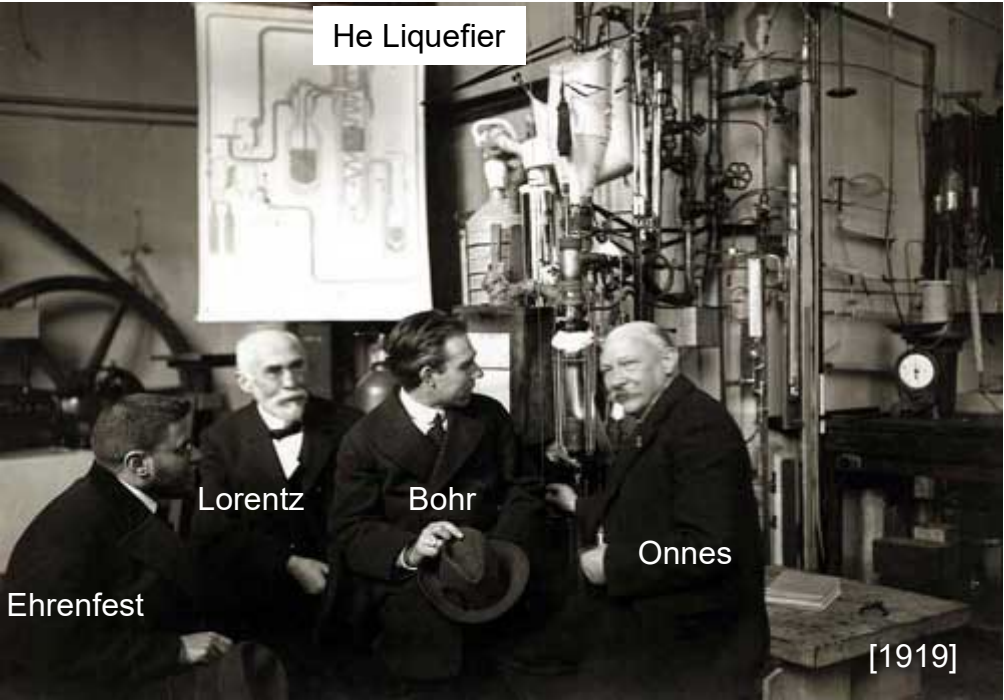
Introduction to Superconductivity & Device Application with Quantum Materials

Gil-Ho Lee

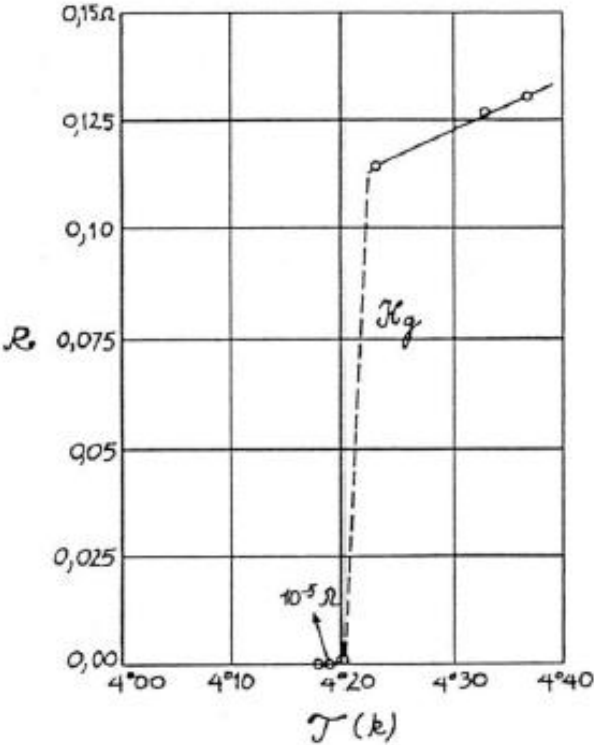
Dept. of Physics, POSTECH, Korea

Basics of Superconductivity & Josephson Junction

Superconductivity

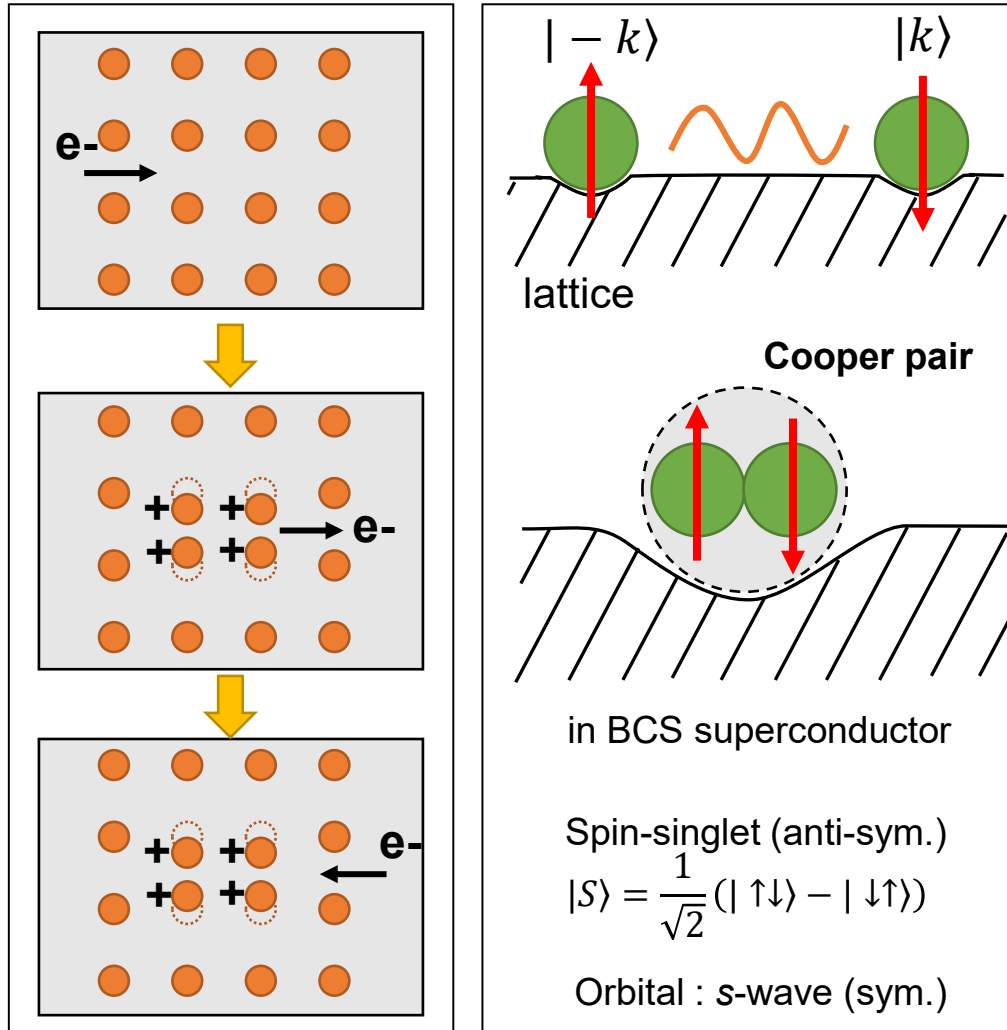


Superconductivity of Mercury (1911)



Superconductivity: Macroscopic Quantum Phenomena

Microscopic mechanism – BCS theory (1957)

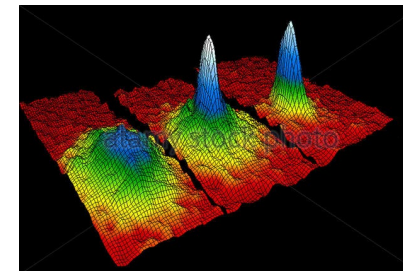


Macroscopic quantum phenomena

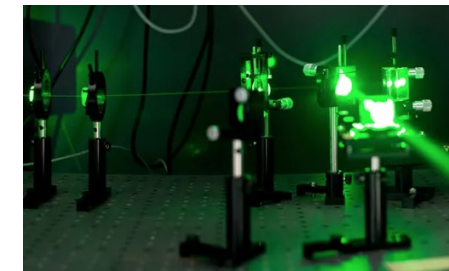
10^{23} -electrons in superconductor behaves as a single quantum object



BEC condensate of atoms



Laser



Quantum Electronics

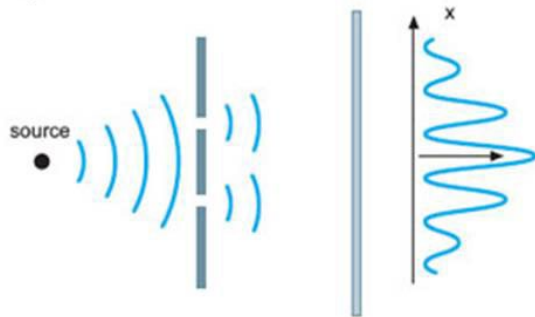
Fundamental Science

Classical Mechanics

Electromagnetics

Quantum Mechanics

e.g.) quantum coherence,
superconductivity



Applied Science

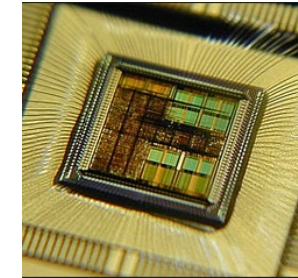
Mechanical Engineering

Electrical Engineering

Quantum Engineering



ex.) Mechanical Engine



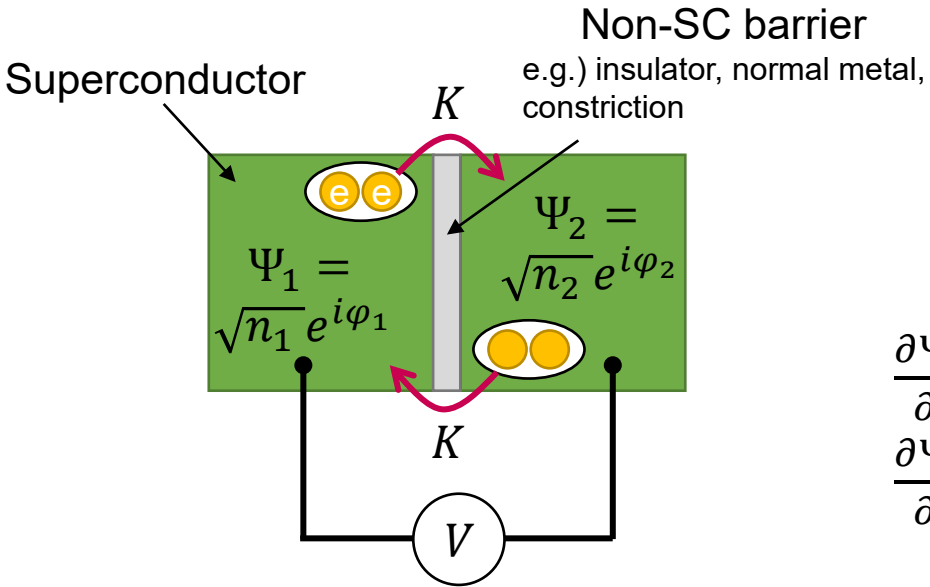
ex.) CPU



ex.) Quantum Computers

Tunneling Josephson Junction (JJ)

Predicted by B. D. Josephson in 1962



n : density of Cooper pair
 φ : phase of order parameter
 K : Coupling parameter

Equation of motion for JJ

$$U_1 - U_2 = qV$$

$$q = 2e$$

$$\begin{cases} i\hbar \frac{\partial \Psi_1}{\partial t} = U_1 \Psi_1 - K \Psi_2 \\ i\hbar \frac{\partial \Psi_2}{\partial t} = U_2 \Psi_2 - K \Psi_1 \end{cases}$$

We set $\frac{U_1 + U_2}{2} = 0$, then $U_1 = \frac{qV}{2}$, $U_2 = -\frac{qV}{2}$

$$\frac{\partial \Psi_1}{\partial t} = \frac{1}{2\sqrt{n_1}} e^{i\varphi_1} \frac{dn_1}{dt} + i\sqrt{n_1} e^{i\varphi_1} \frac{d\varphi_1}{dt} = \frac{qV}{2i\hbar} \sqrt{n_1} e^{i\varphi_1} - \frac{K}{i\hbar} \sqrt{n_2} e^{i\varphi_2} - \text{Eq. (1)}$$

$$\frac{\partial \Psi_2}{\partial t} = \frac{1}{2\sqrt{n_2}} e^{i\varphi_2} \frac{dn_2}{dt} + i\sqrt{n_2} e^{i\varphi_2} \frac{d\varphi_2}{dt} = -\frac{qV}{2i\hbar} \sqrt{n_2} e^{i\varphi_2} - \frac{K}{i\hbar} \sqrt{n_1} e^{i\varphi_1} - \text{Eq. (2)}$$



(1) $\times e^{-i\varphi_1}$, (2) $\times e^{-i\varphi_2}$

Phase difference: $\varphi \equiv \varphi_2 - \varphi_1$

$$\frac{1}{2\sqrt{n_1}} \frac{dn_1}{dt} + i\sqrt{n_1} \frac{d\varphi_1}{dt} = -i \frac{qV}{2\hbar} \sqrt{n_1} + i \frac{K}{\hbar} \sqrt{n_2} e^{i(\varphi_2 - \varphi_1)} - \text{Eq. (1)'}$$

$$\frac{1}{2\sqrt{n_2}} \frac{dn_2}{dt} + i\sqrt{n_2} \frac{d\varphi_2}{dt} = +i \frac{qV}{2\hbar} \sqrt{n_2} + i \frac{K}{\hbar} \sqrt{n_1} e^{-i(\varphi_2 - \varphi_1)} - \text{Eq. (2)'}$$

DC & AC Josephson Relationship

by using $e^{i\varphi} = \cos \varphi + i \sin \varphi$,

$$\frac{1}{2\sqrt{n_1}} \frac{dn_1}{dt} + i\sqrt{n_1} \frac{d\varphi_1}{dt} = -i \frac{qV}{2\hbar} \sqrt{n_1} + i \frac{K}{\hbar} \sqrt{n_2} (\cos \varphi + i \sin \varphi) \text{ - Eq. (1)''}$$

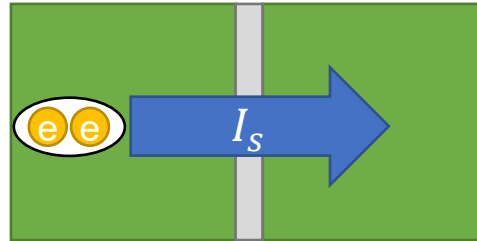
$$\frac{1}{2\sqrt{n_2}} \frac{dn_2}{dt} + i\sqrt{n_2} \frac{d\varphi_2}{dt} = +i \frac{qV}{2\hbar} \sqrt{n_2} + i \frac{K}{\hbar} \sqrt{n_1} (\cos \varphi - i \sin \varphi) \text{ - Eq. (2)''}$$

- Real part of Eqs. (1)'' and (2)''

$$\frac{dn_1}{dt} = -2 \frac{K}{\hbar} \sqrt{n_1 n_2} \sin \varphi$$

Supercurrent:

$$I_s \propto -\frac{dn_1}{dt} = \frac{dn_2}{dt}$$



DC Josephson relationship

$$I_s = I_c \sin \varphi$$

$$\frac{dn_2}{dt} = +2 \frac{K}{\hbar} \sqrt{n_1 n_2} \sin \varphi$$

- Imaginary part of Eqs. (1)'' and (2)''

$$\frac{d\varphi_1}{dt} = -\frac{qV}{2\hbar} + \frac{K}{\hbar} \sqrt{\frac{n_2}{n_1}} \cos \varphi$$

If $n_1 \approx n_2$,

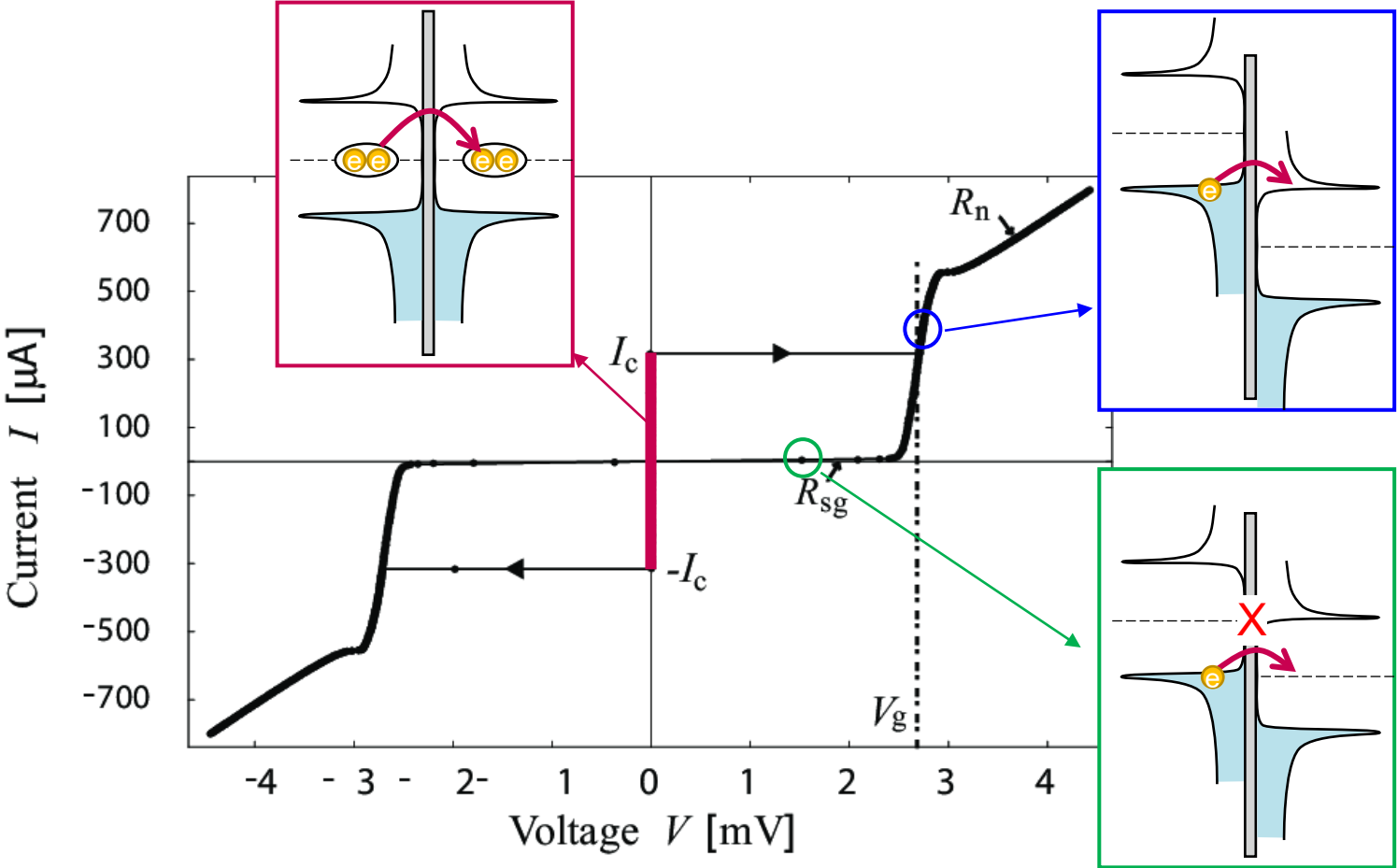
$$\frac{d\varphi}{dt} = \frac{d\varphi_2}{dt} - \frac{d\varphi_1}{dt} = \frac{qV}{\hbar} = \frac{2eV}{\hbar}$$

$$\frac{d\varphi_2}{dt} = \frac{qV}{2\hbar} + \frac{K}{\hbar} \sqrt{\frac{n_1}{n_2}} \cos \varphi$$

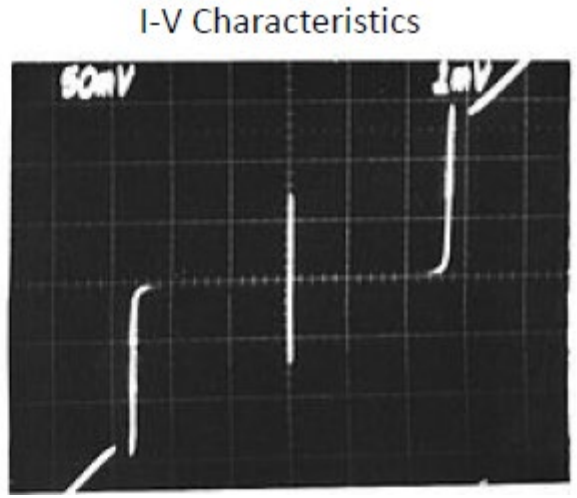
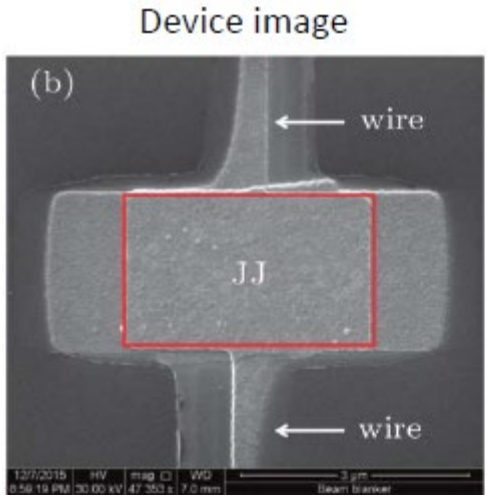
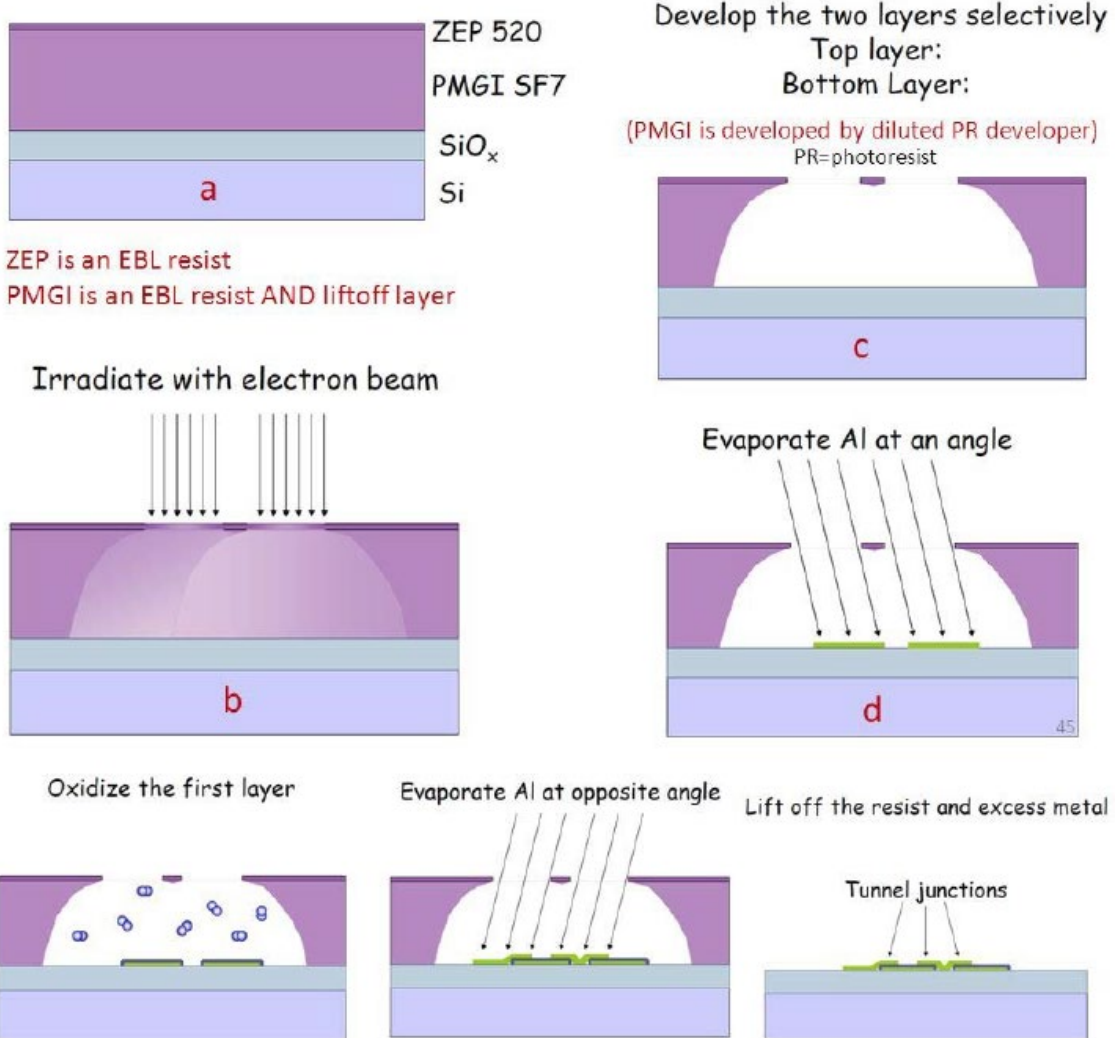
AC Josephson relationship

$$\frac{d\varphi}{dt} = \frac{2e}{\hbar} V$$

Typical Current-Voltage Characteristics of JJ

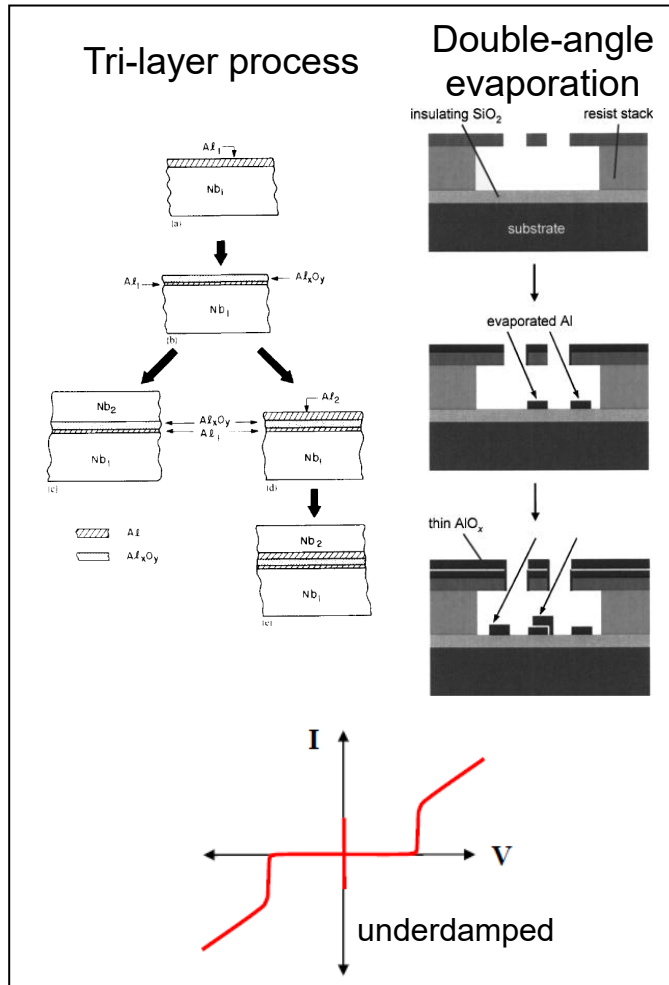


Angle Evaporation for Tunneling JJ

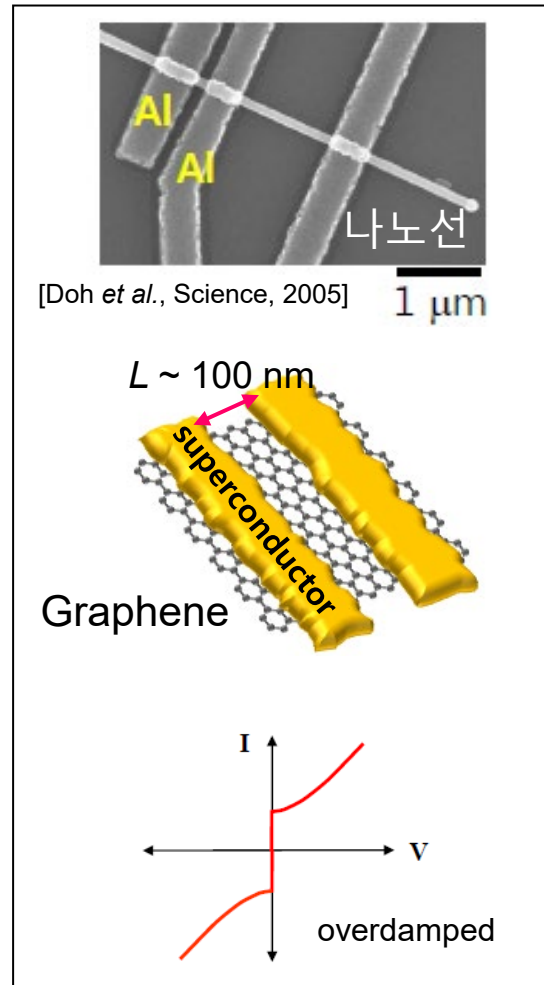


Various types of Josephson Junctions

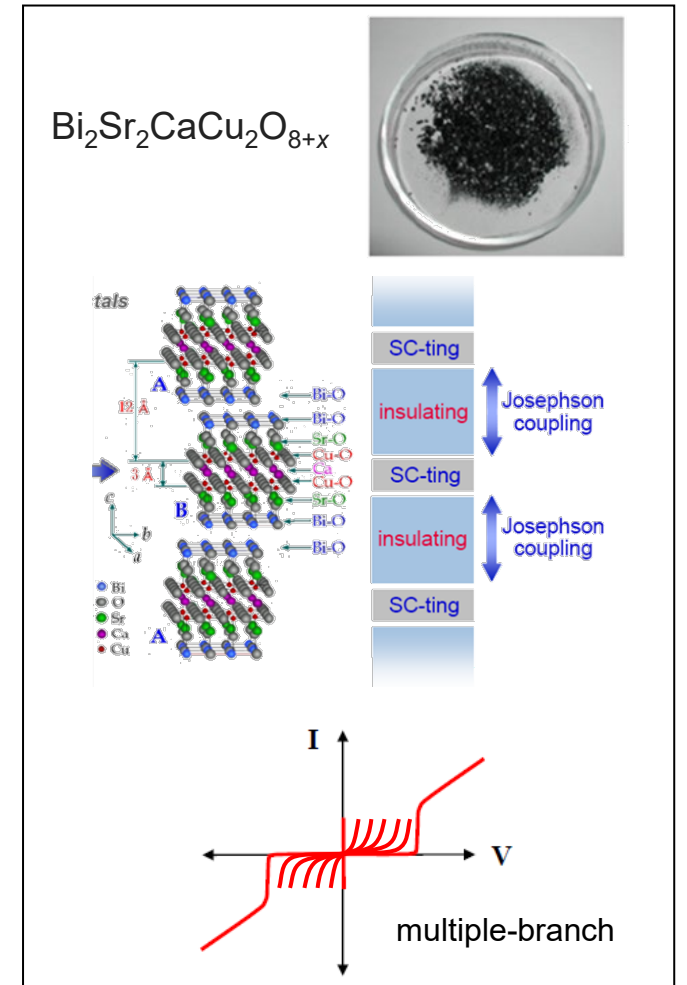
투과형 조셉슨 접합
(tunneling Josephson junction)



근접형 조셉슨 접합
(proximity Josephson junction)

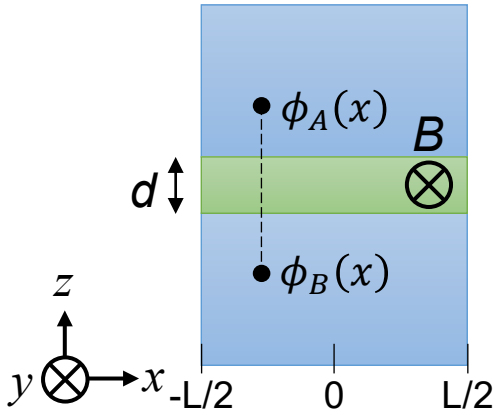


선천성 조셉슨 접합
(intrinsic Josephson junction)



Fraunhofer Pattern

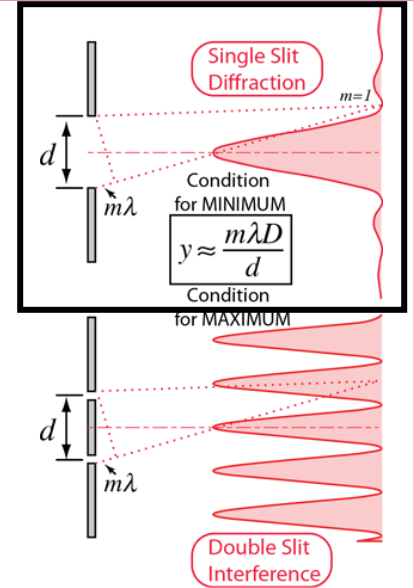
- With external magnetic field $B\hat{y}$,



- Phase difference: $\phi(x) \equiv \phi_B(x) - \phi_A(x)$
- $\phi(x) = \phi(0) + 2\pi(Bd/\Phi_0)x$
- Overall Josephson current:

$$I_J(\Phi) = \int_{-L/2}^{L/2} dx J(x) \sin[\phi(x)].$$

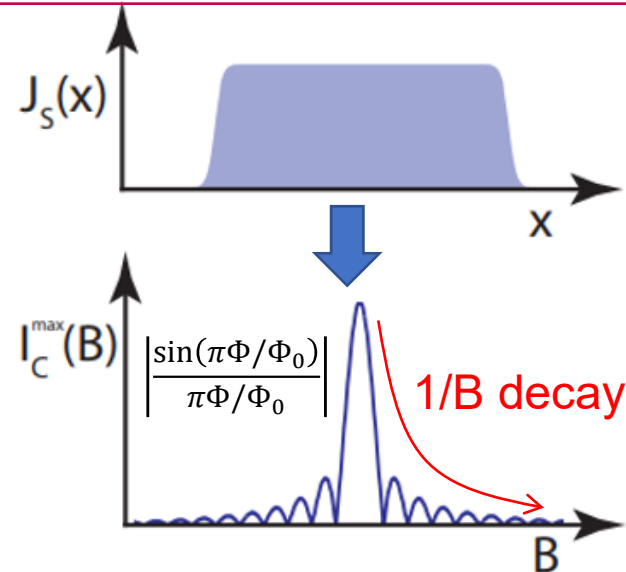
↑
Josephson current density



- For **uniform** Josephson coupling [$J(x) = \text{'constant'}$],

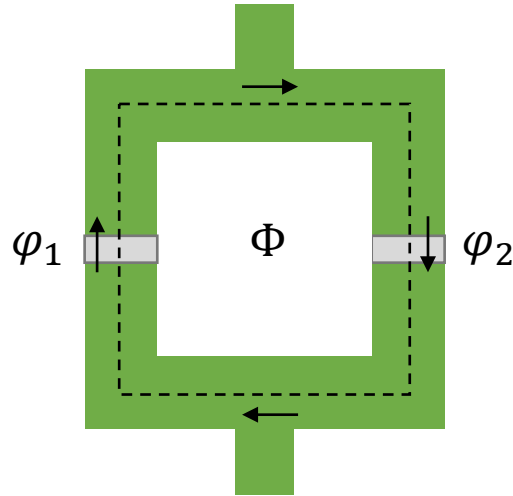
Critical current: $I_c(\Phi) = \max_{\phi(0)} \{I_J(\Phi)\} = I_c \left| \frac{\sin \alpha}{\alpha} \right|$

with reduced external flux $\alpha = \pi\Phi/\Phi_0$, $\Phi = BdL$



SQUID (Superconducting Interference Device)

Two JJs connected in parallel



$$\varphi_{\text{total}} = \varphi_2 - \varphi_1 + 2\pi \frac{\Phi}{\Phi_S} = 2\pi n$$

$$\varphi_1 - \varphi_2 = 2\pi \frac{\Phi}{\Phi_S} \pmod{2\pi}$$

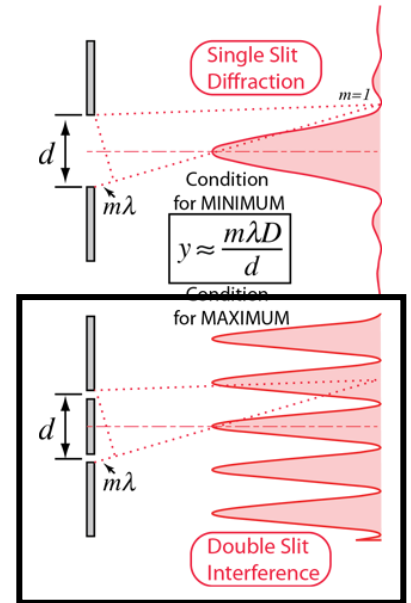
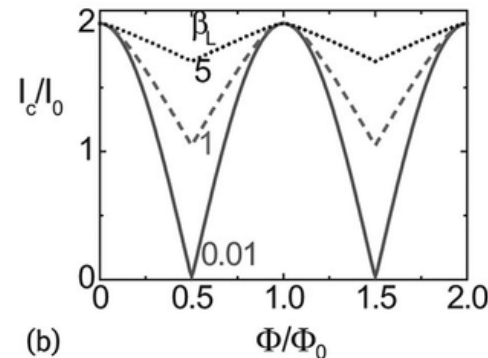
Φ : external magnetic flux threading SQUID loop
 $\Phi_S = h/2e$: flux quantum for Cooper pairs
 n : integer number

- Supercurrent through SQUID:

$$\begin{aligned} I_{s,\text{SQ}} &= I_c \sin \varphi_1 + I_c \sin \left(\varphi_1 - 2\pi \frac{\Phi}{\Phi_S} \right) \\ &= 2I_c \cos \left(\frac{\pi\Phi}{\Phi_S} \right) \sin \left(\varphi_1 - \pi \frac{\Phi}{\Phi_S} \right) \end{aligned}$$

- Critical current for SQUID:

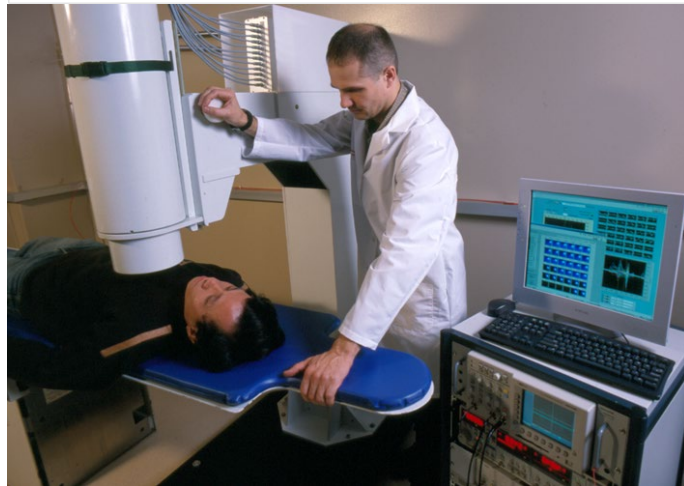
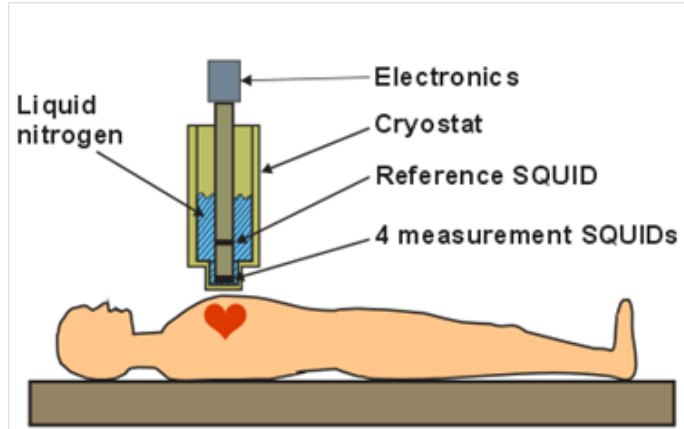
$$I_{c,\text{SQ}} = \max_{\varphi_1} I_{s,\text{SQ}}(\varphi_1) = 2I_c \left| \cos \left(\frac{\pi\Phi}{\Phi_S} \right) \right|$$



For 1 mm x 1 mm SQUID,
 Φ_S corresponds to 20 μG .
 \downarrow
 SQUID can be used as
 a very sensitive magnetometer

MCG (심자도) & MEG (뇌자도)

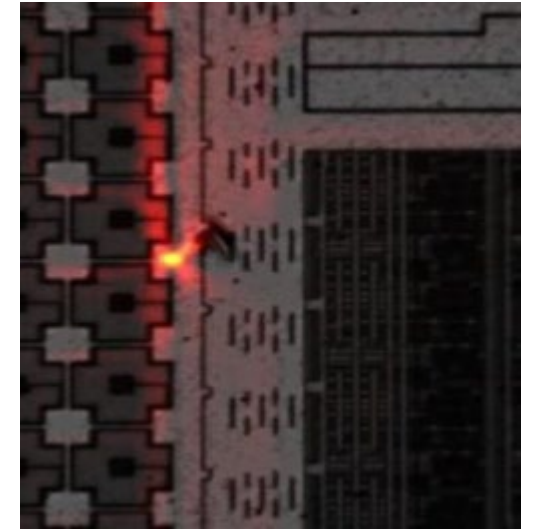
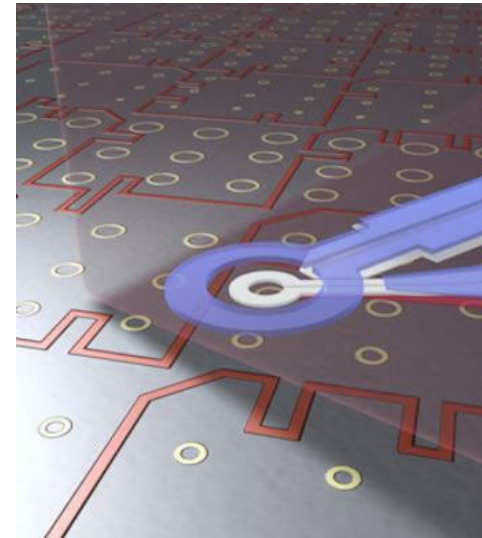
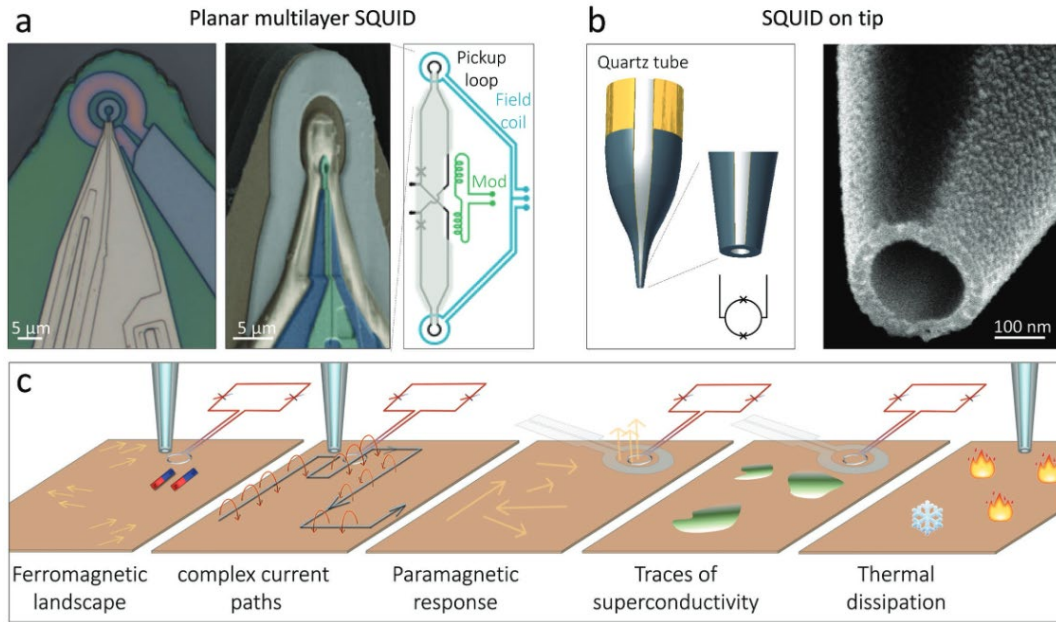
Magneto-Cardio-Graphy (MCG)



Magneto-Encephalo-Graphy (MEG)



Scanning SQUID Microscope

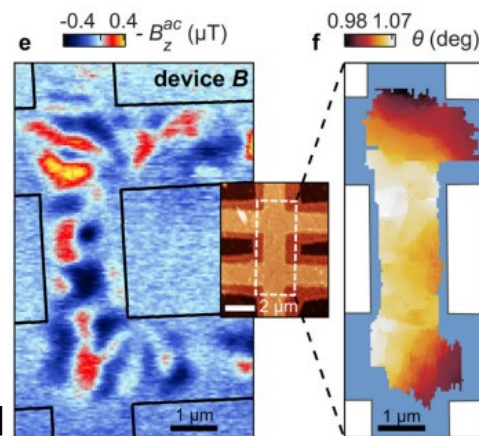


Non-invasive
Circuit Failure Analysis

Commercial product by Nocera

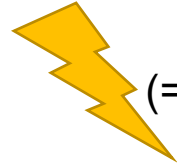
e.x.) mapping twist angle of magic angle twisted bilayer graphene

[Nature 581, 47–52 (2020)]

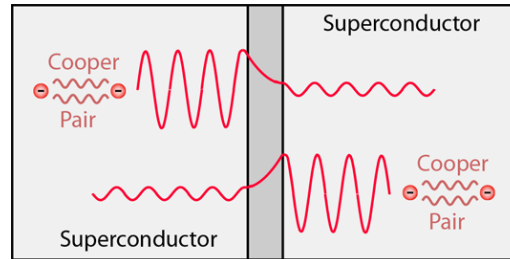


Shapiro step (1963)

$$V(t) = V_{ac} \cos \omega t$$



Microwave
(= AC voltage biasing)



$$\frac{d\phi(t)}{dt} = \frac{2eV(t)}{\hbar}$$

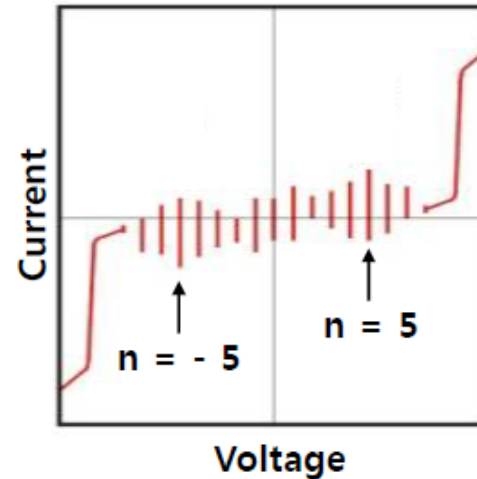
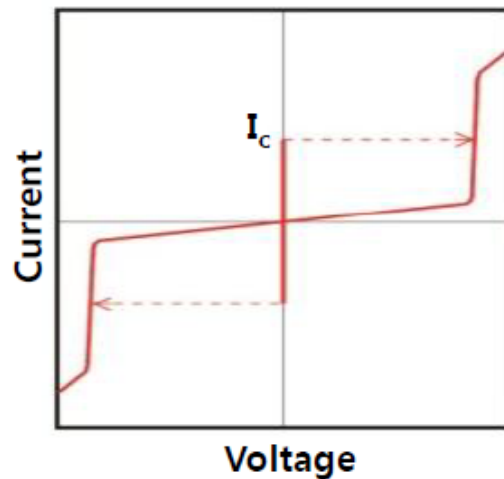
$$\phi(t) \propto \sin \omega t$$

$$I_J = I_c \sin(\phi(t)) \propto \sin(\sin \omega t)$$



Resonance of Josephson junction with microwave

$$V_n = n \frac{\hbar \omega}{2e} \quad (n = \text{integer})$$



“AC→DC converter”

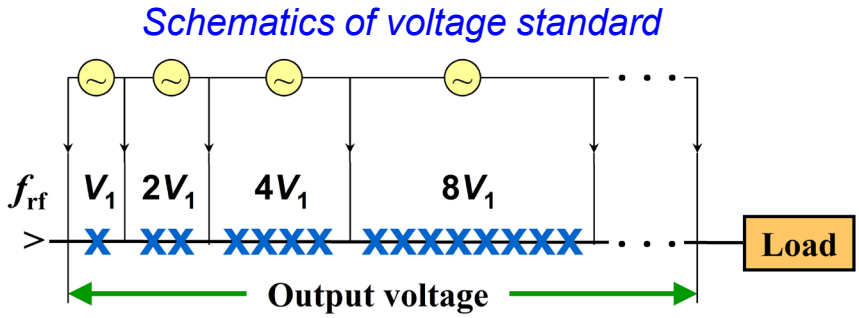
Voltage standard “AC→DC”

$$V_n = n \frac{\hbar\omega}{2e} \quad (n=\text{integer})$$

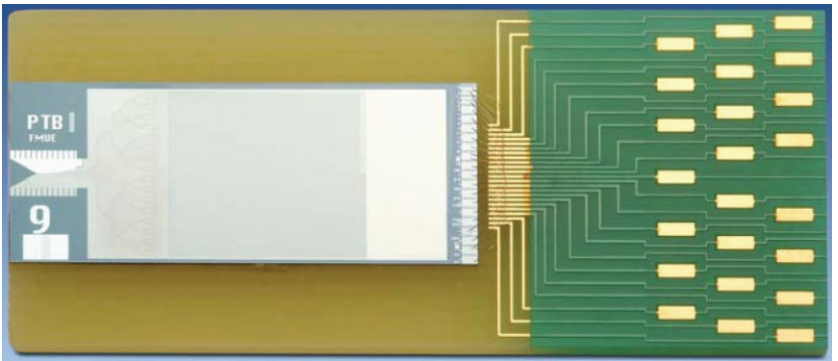
Fundamental constant

$\sim 2.06783385 \dots \mu\text{V}/\text{GHz}$

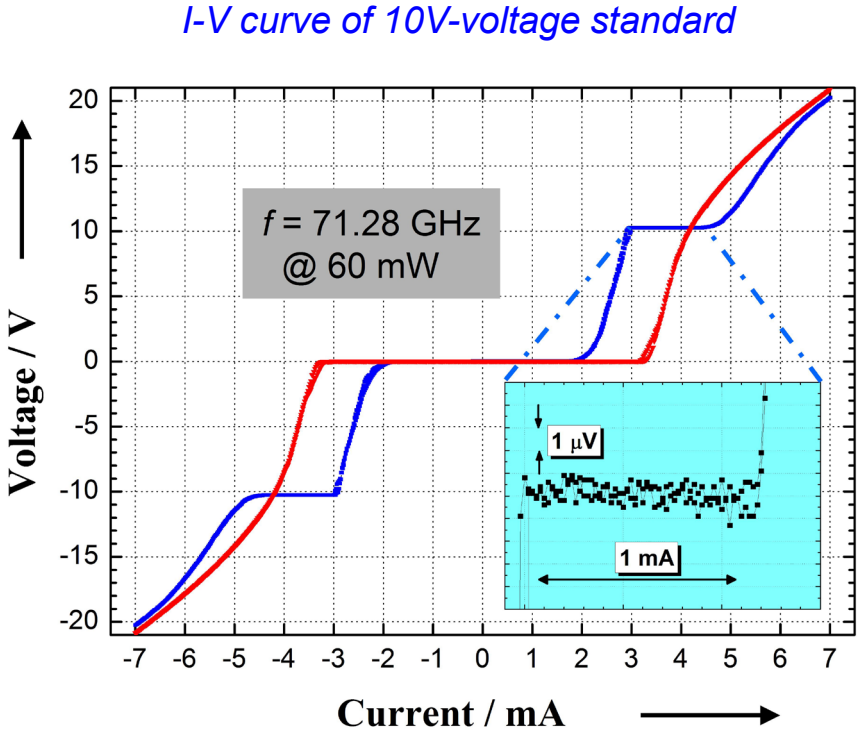
Generation of precise voltage using Shapiro steps



~ Array consisting of 70,000 Josephson junctions

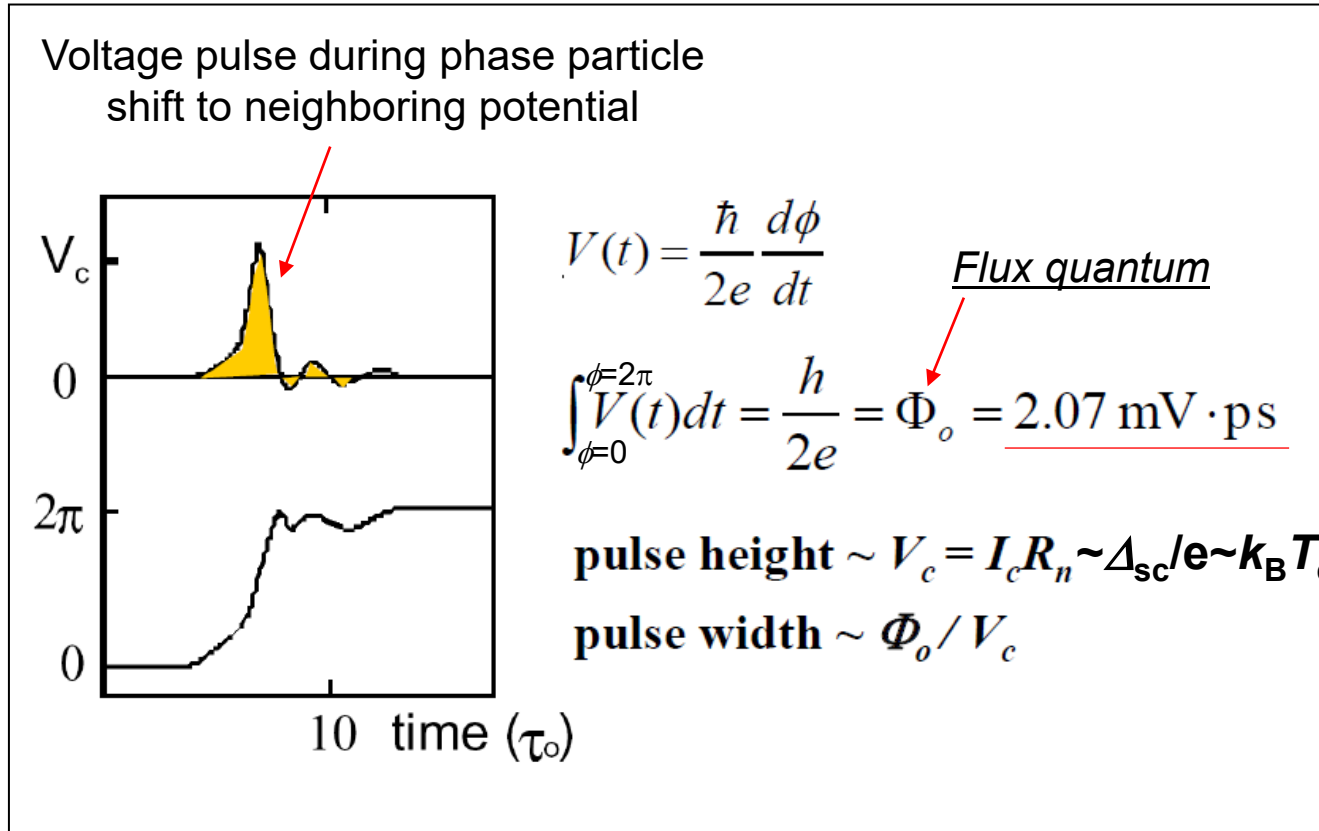
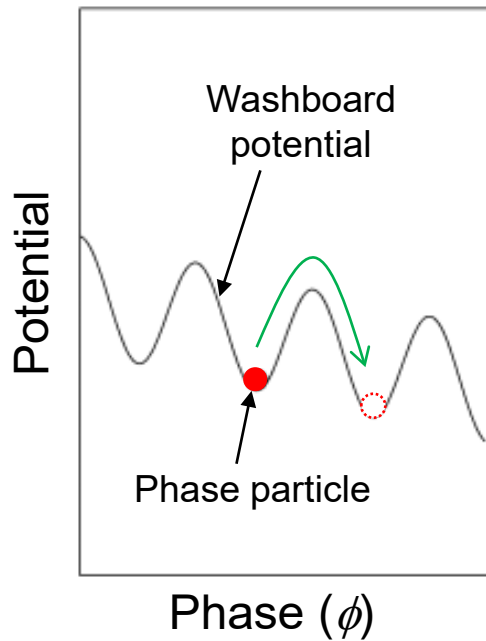


[F. Mueller et al. (2009)]



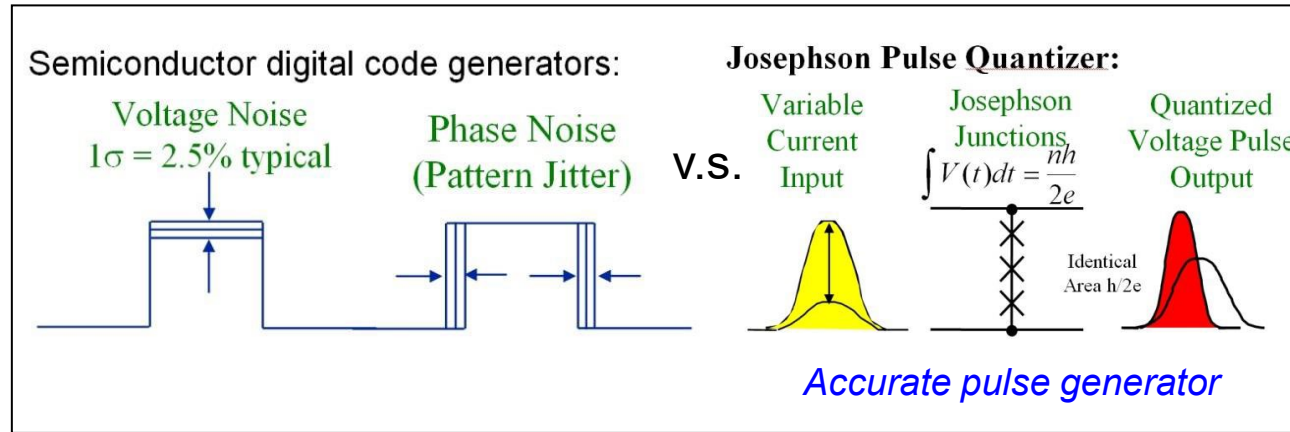
Josephson Voltage Pulse

Generation of rapid and precise voltage pulse of ~1 ps

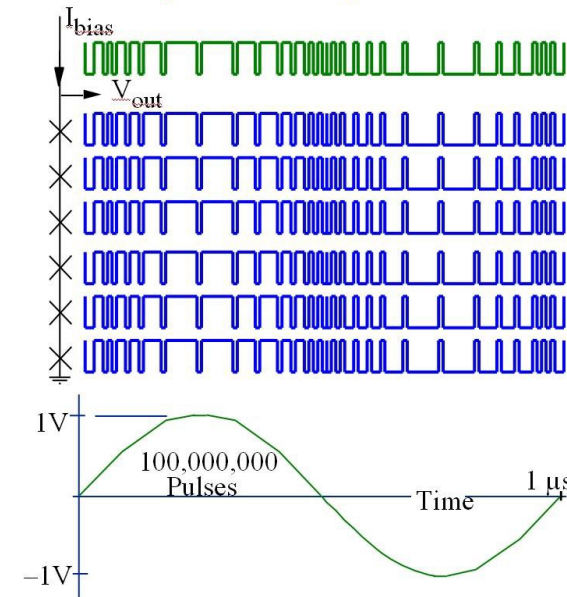


JAWS & RSFQ

Josephson Arbitrary Waveform Synthesizer (JAWS)



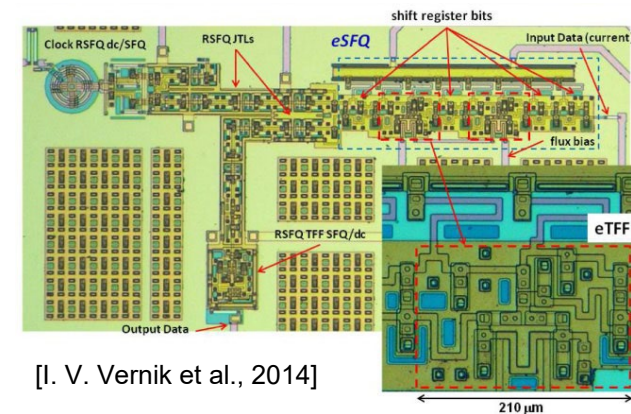
Digital-to-Analog Conversion



Rapid single flux quantum (RSFQ)

- Digital logic device using Josephson pulse instead of 0/5 V TTL
- Data encoding, processing, transmitting with 1ps pulse
 - Fast processing (**100 GHz** clock speed)
- Superconducting transmission line
 - Much less heating problem

RFSQ device



[I. V. Vernik et al., 2014]

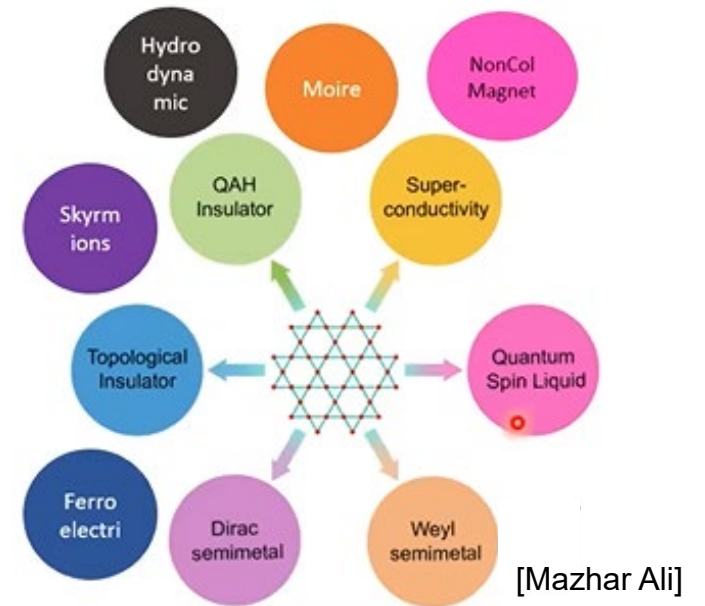
Van der Waals Material based Superconducting devices

Quantum Materials / Van der Waals Materials



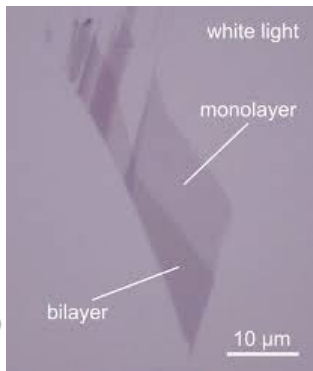
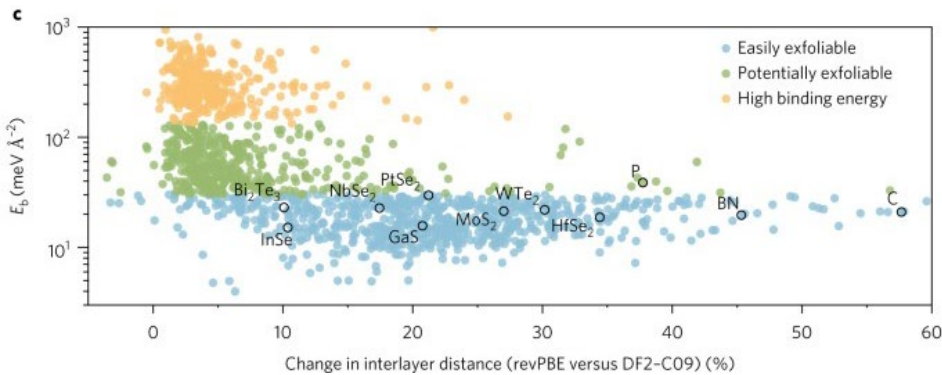
Quantum material- a material whose properties are not best described using classical particles or calculations that do not take into account the full character of the system.

- Topological materials
- Spin liquids
- Superconductors
- Non-collinear magnets
- Strongly correlated materials

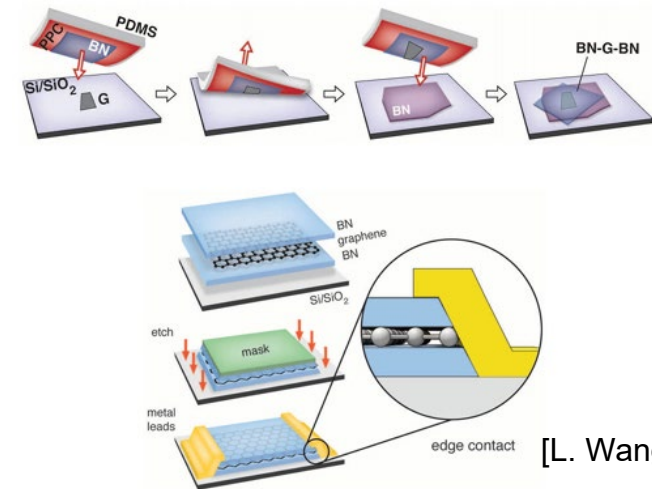


[Journal of Physics D: Applied Physics 51 (2020)]

[Mazhar Ali]



[N. Mounet et al., Nat. Nanotechnol. 13, 246-252 (2018)]

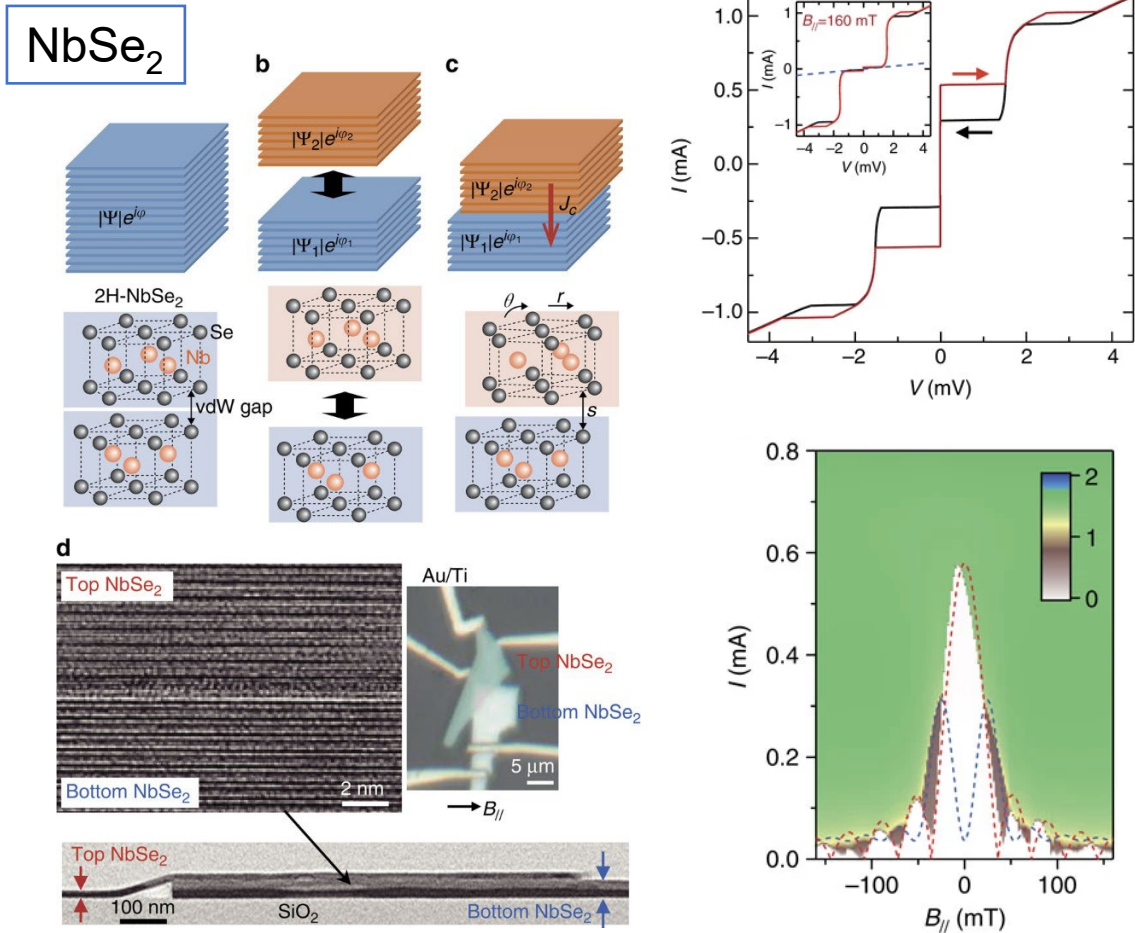


vdW stacking technique

‘Relatively’ easy to make devices

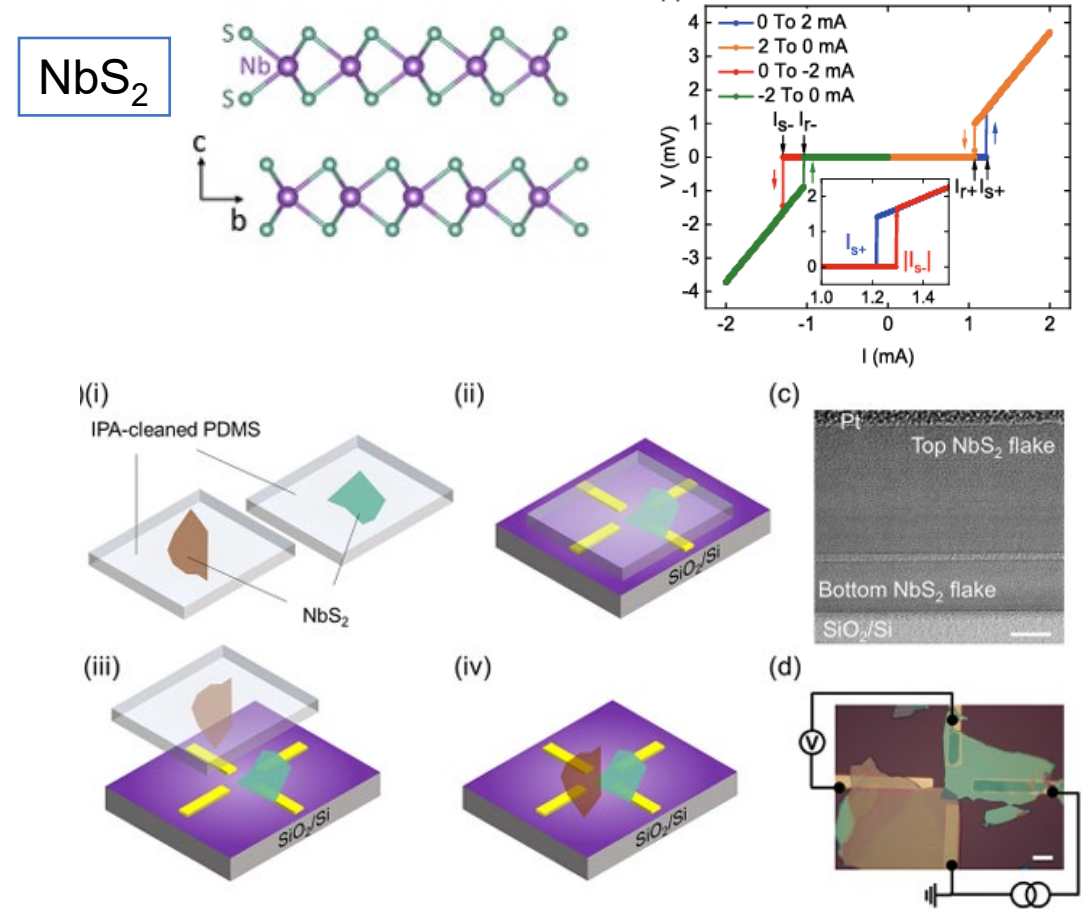
[L. Wang et al., Science 342, 614 (2013)]

vdW-based Josephson Junctions (1)



- Exfoliated and transferred in air in < 1 hour

[N. Yabuki et al., Nat. Comm. 7, 10616 (2016)]

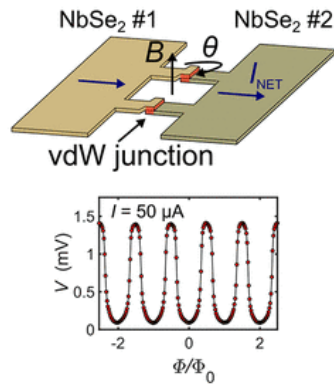
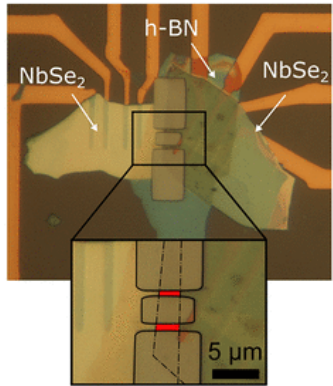
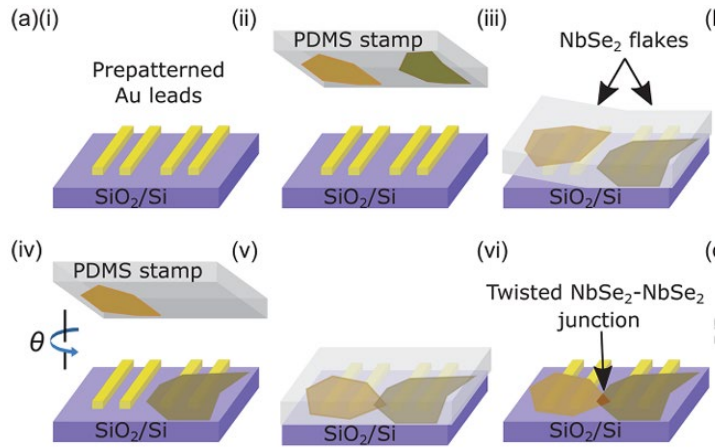


- Dry-transfer in a glovebox

[C. Zhao et al., J. Phys. Chem. Lett. 2022, 13, 46, 10811 (2022)]

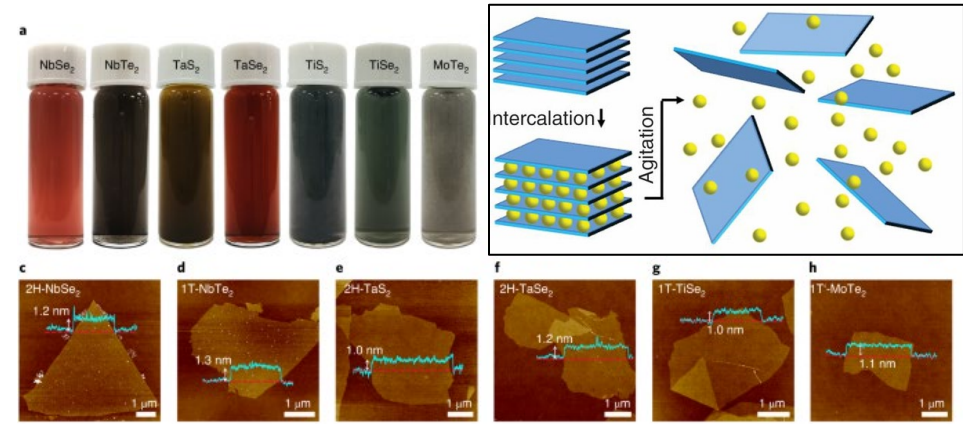
vdW-based SQUID

NbSe₂



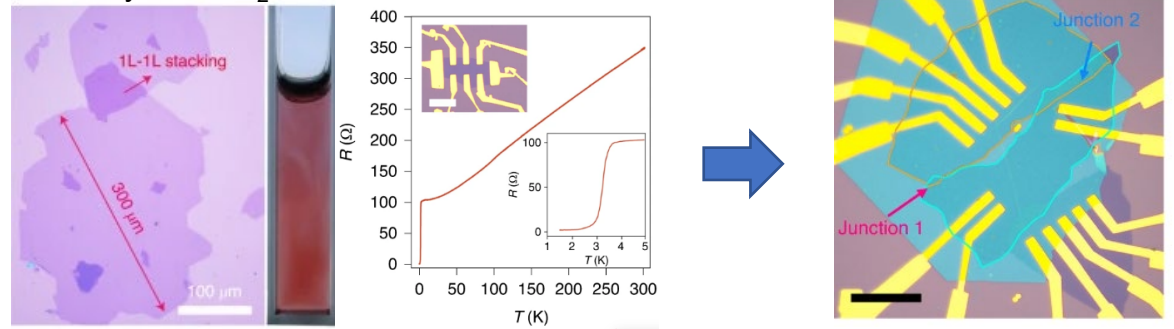
- Demonstration of vdW-based SQUID device

[L. S. Farrar et al., Nano Lett. 21, 6725 (2021)]



electrochemical exfoliation of bulk TMDs to 2D SC

Monolayer NbSe₂

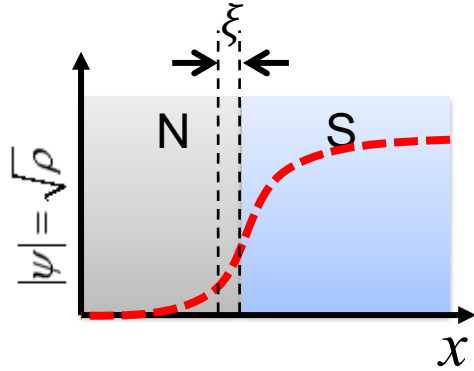


solvent protection prevents air degradation

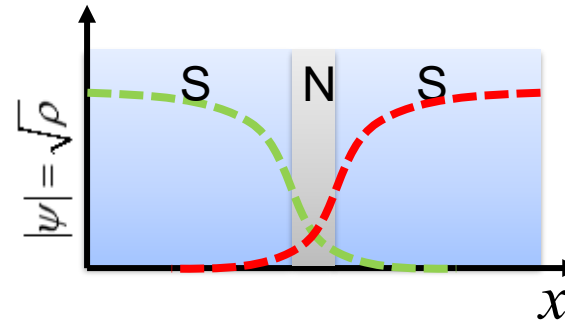
[J. Li et al., Nat. Mater. 20, 181 (2021)]

Proximity Josephson Junction

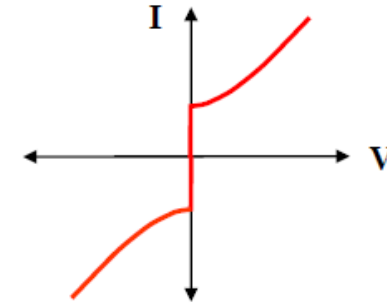
In mesoscopic point of view,



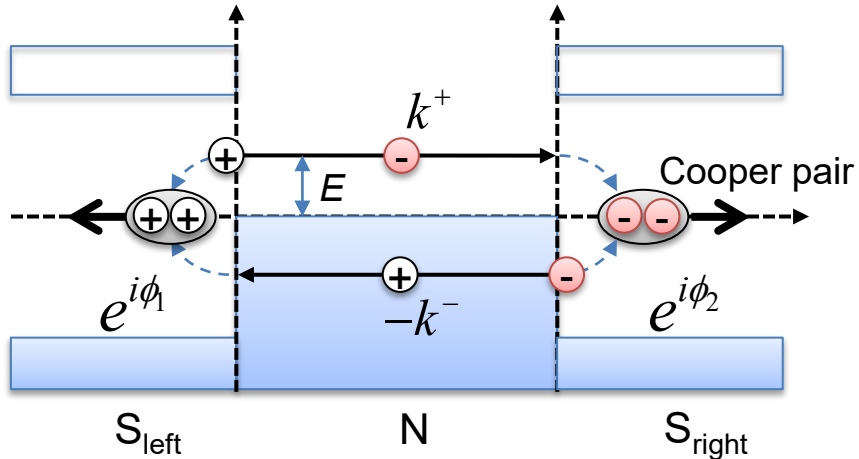
Proximity effect



Proximity Josephson coupling



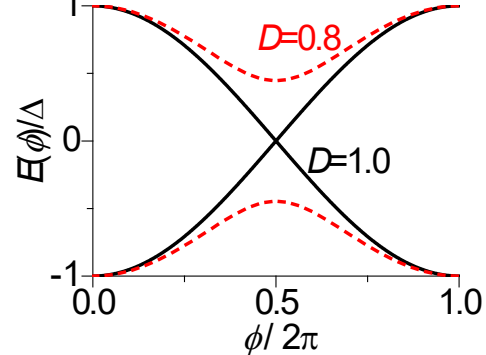
In microscopic point of view,



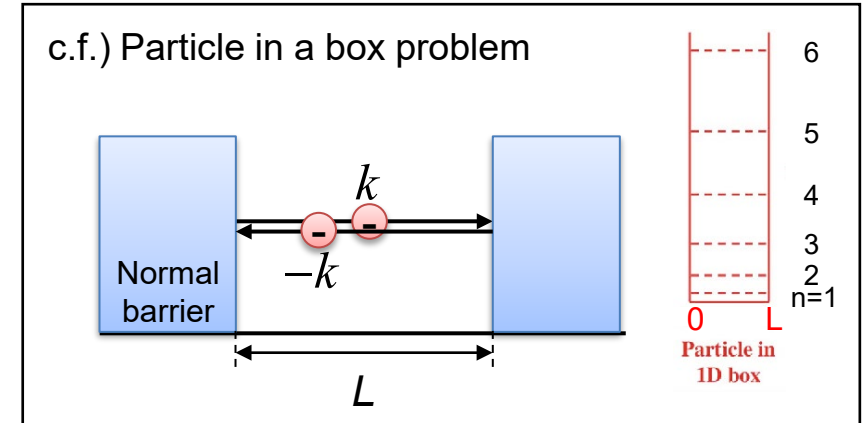
Bohr-Sommerfeld quantization:

$$2 \cos^{-1} \left(\frac{E}{\Delta} \right) + k^+ L + (-k^- L) \pm \phi = 2\pi n$$

Andreev bound state (ABS)

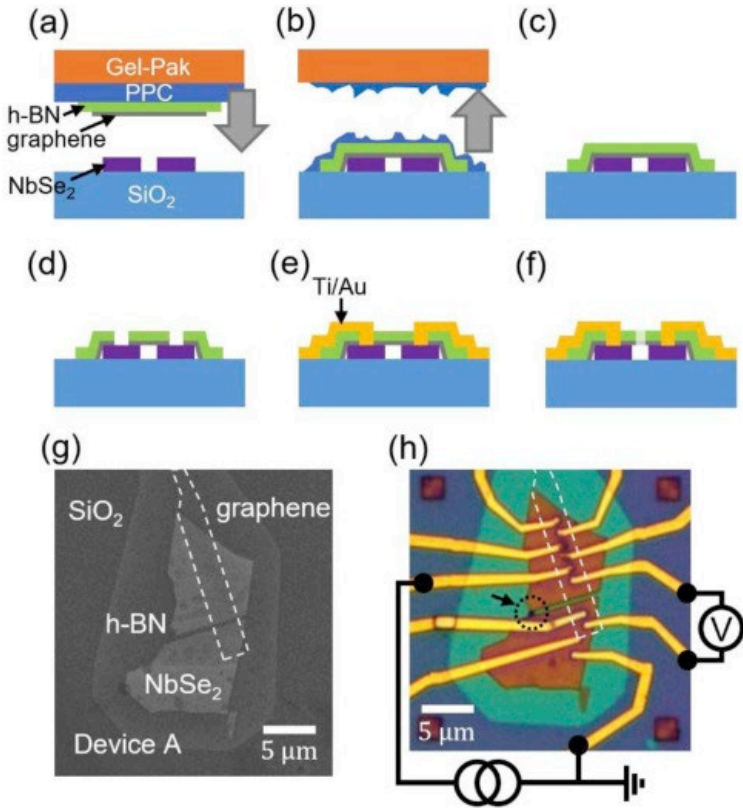


c.f.) Particle in a box problem

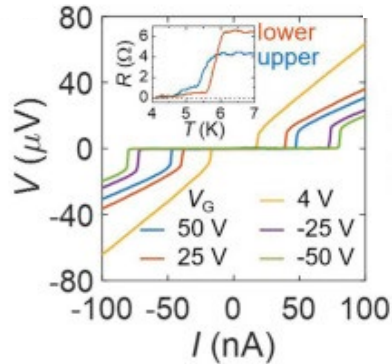


NbSe₂/Graphene/NbSe₂

Planar Josephson junction

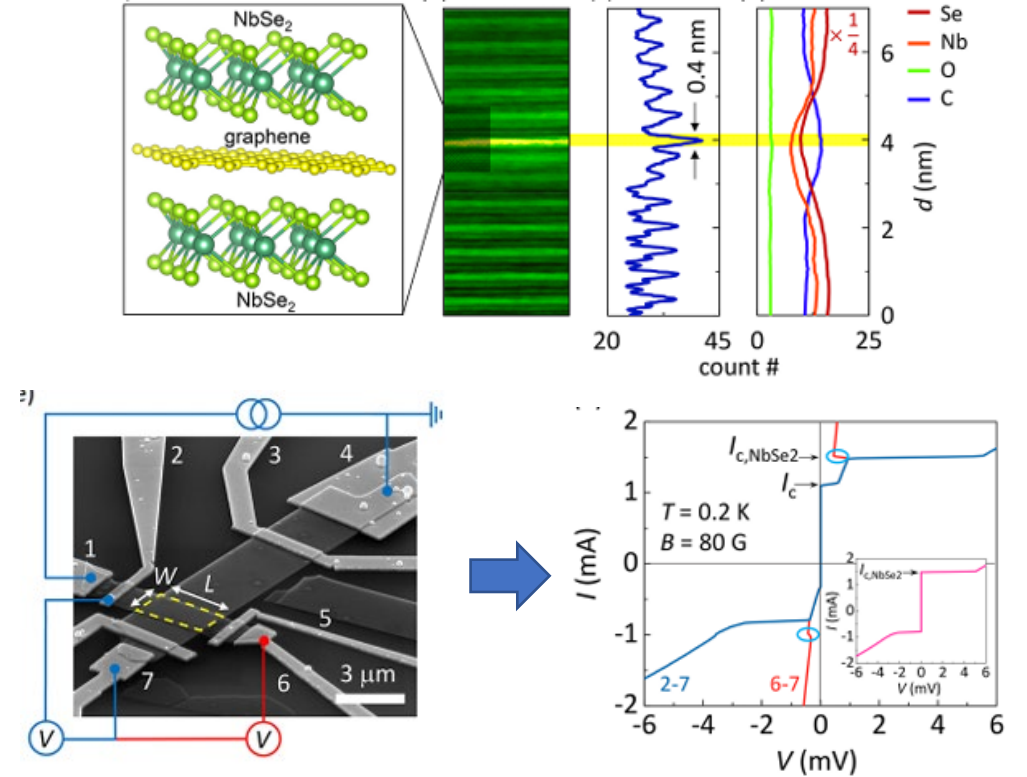


- Full vdW-based JJ
- long-diffusive junction
- $I_c R_N \sim 10 \mu V$
- $\Delta_{NbSe_2} \sim 0.8 meV$



[Jongyun Lee et al., CAP 19, 251 (2019)]

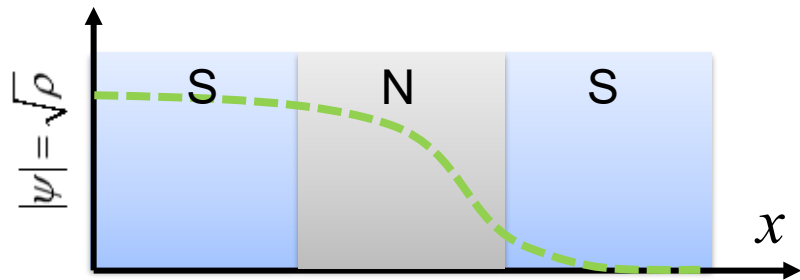
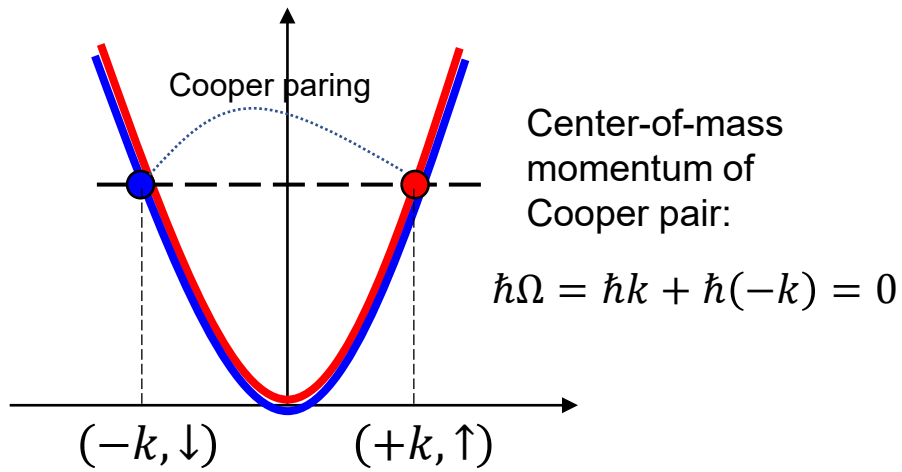
Vertical Josephson junction



- Full vdW-based vertical JJ
- $J_c \sim 10^4 A/m^2$

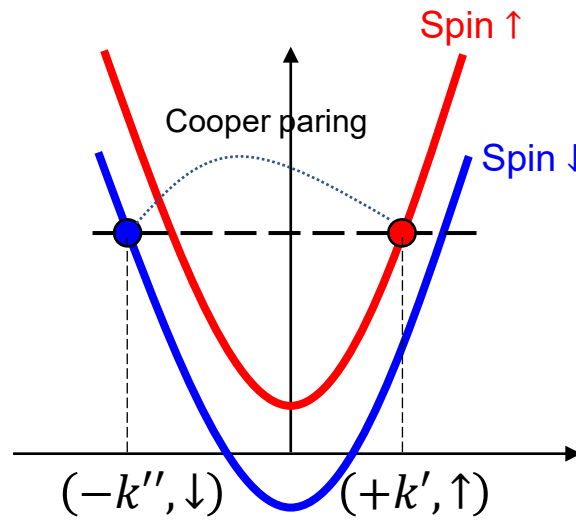
[Minsoo Kim et al., Nano Lett. 17, 6125 (2017)]

π -Josephson junction



0-Josephson junction

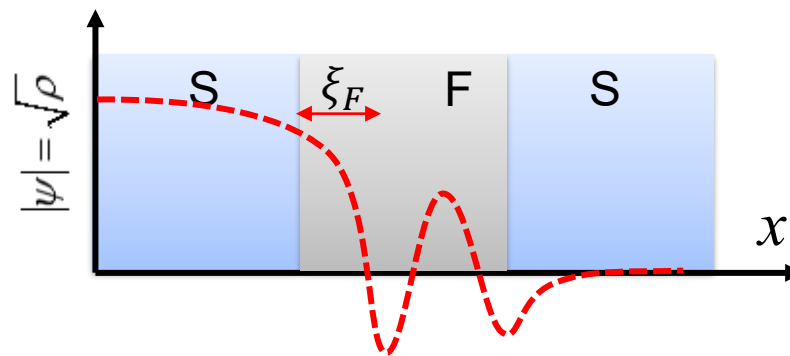
$$I_J = I_c \sin(\phi)$$



$$\hbar\Omega = \hbar k' + \hbar(-k'') \neq 0$$

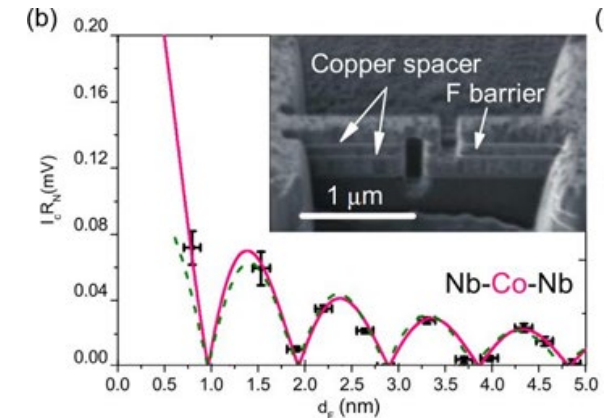
↓

Oscillating term in ψ



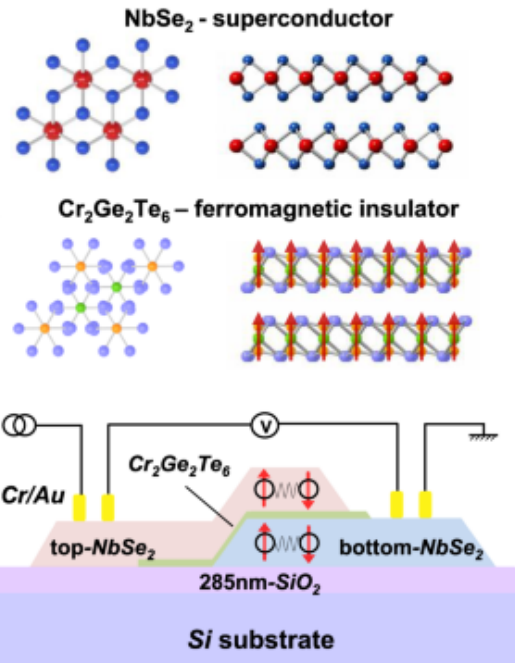
π -Josephson junction

$$I_J = I_c \sin(\phi + \pi) = -I_c \sin(\phi)$$



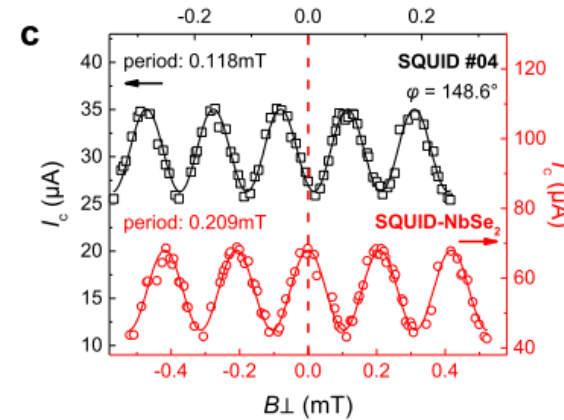
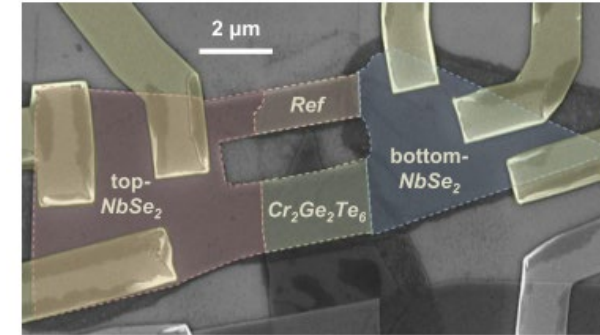
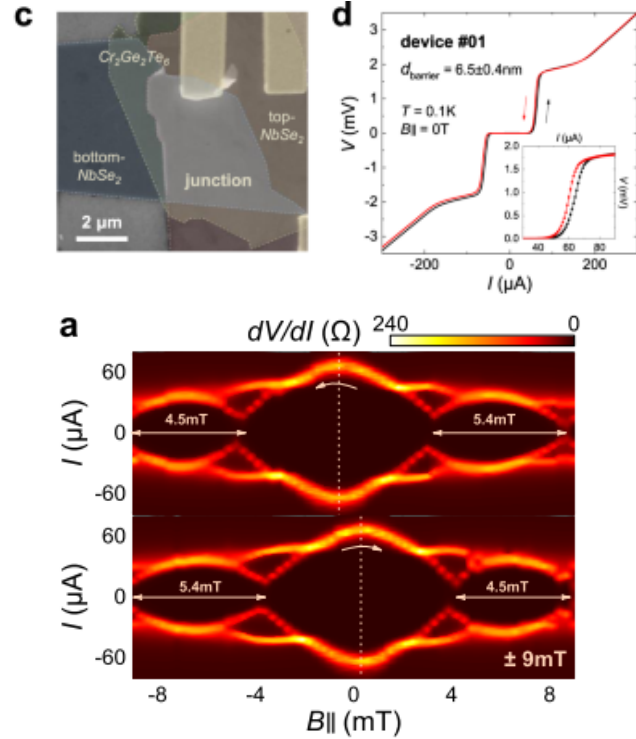
[J. W. A. Robinson et al.,
 PRL 97, 177003 (2006)]

vdW-ferromagnetic Josephson junctions

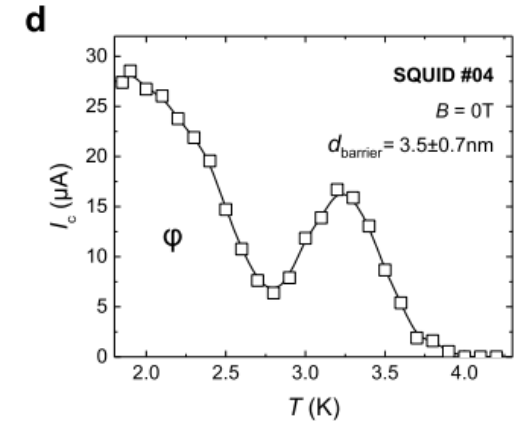


Fabricated in a glovebox

Magnetic hysteresis in Fraunhofer pattern



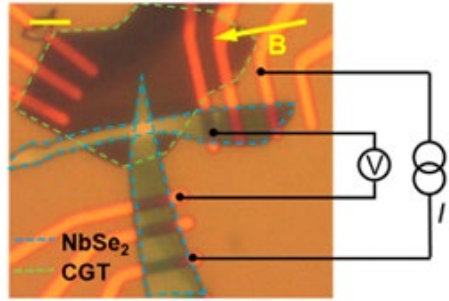
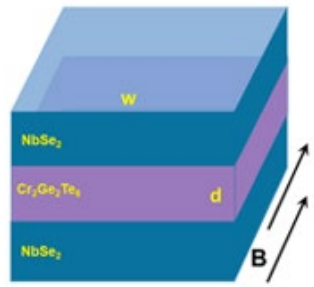
~0.8 π phase shift in SQUID interference



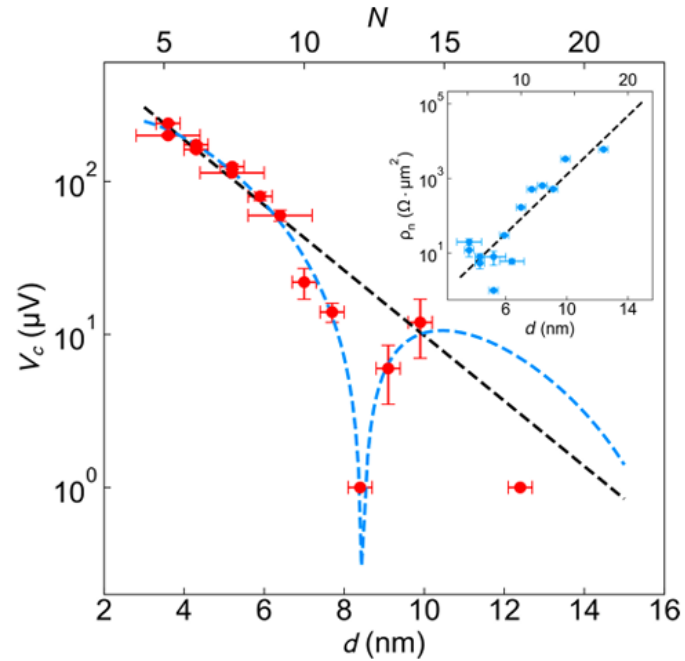
Non-monotonic $I_c(T)$

[Linfeng Ai et al., Nat. Comm. 12, 6580 (2021)]

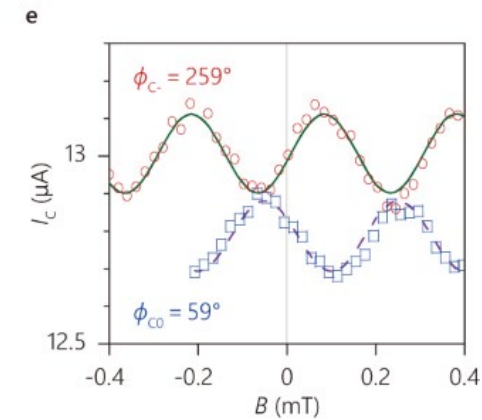
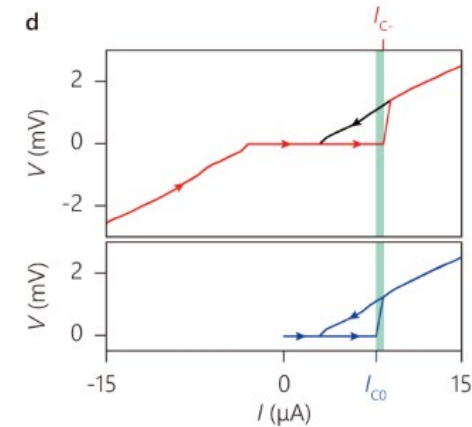
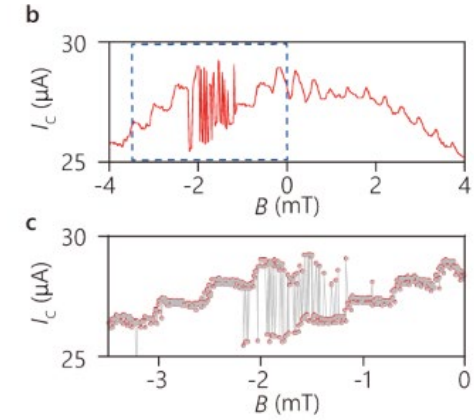
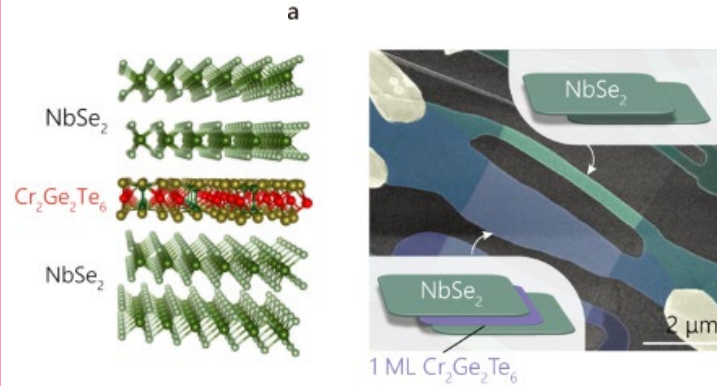
vdW-ferromagnetic Josephson junctions



d_f dependence
of $V_c = I_c R_N$



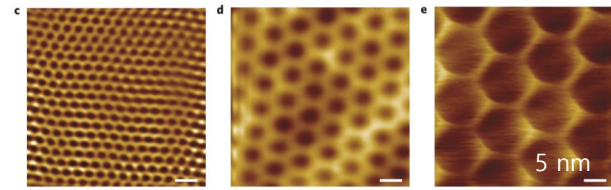
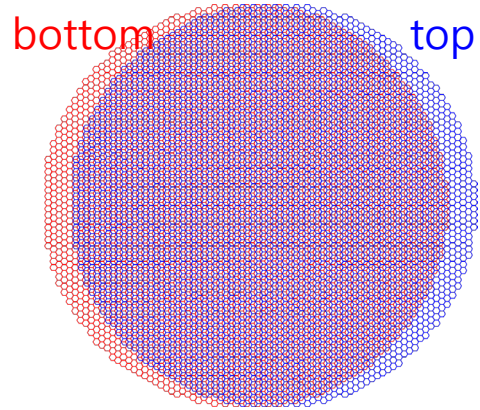
[K. Kang et al., Nano Lett. 22, 5510 (2022)]



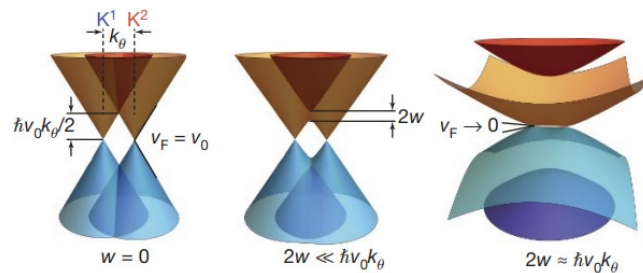
$\sim 1.4 \pi$ and $\sim 0.3 \pi$ phase shift in SQUID interference

[H. Idzuchi et al., Nat. Comm. 12, 5332 (2021)]

Twist-angle Tunable vdW Interfaces

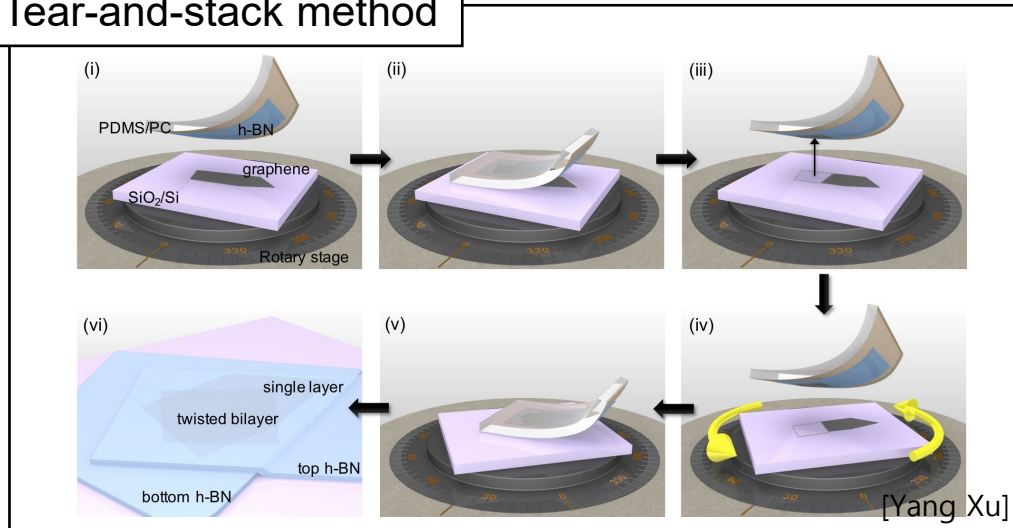


[Nat. Phys. **8**, 382 (2012)]



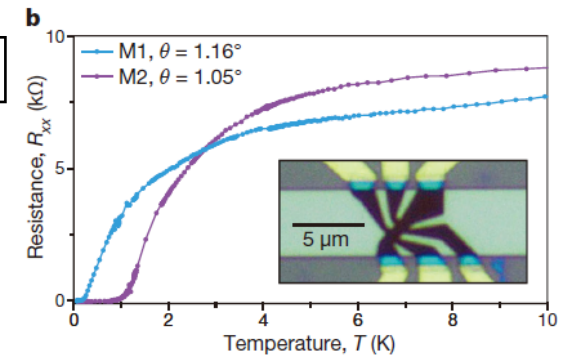
[Nature **556**, 80–84 (2018)]

Tear-and-stack method

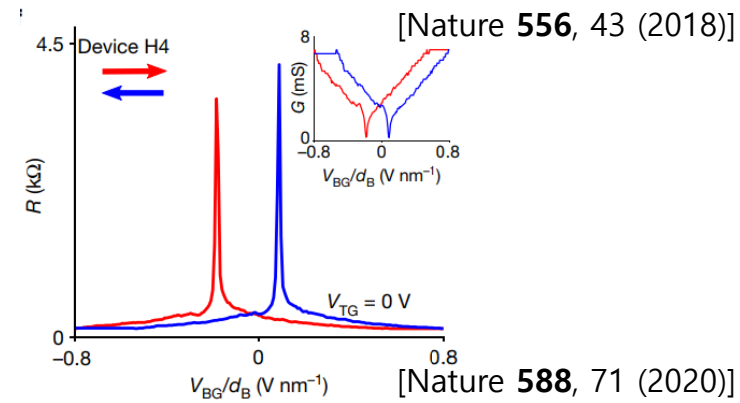


[Yang Xu]

Superconductivity



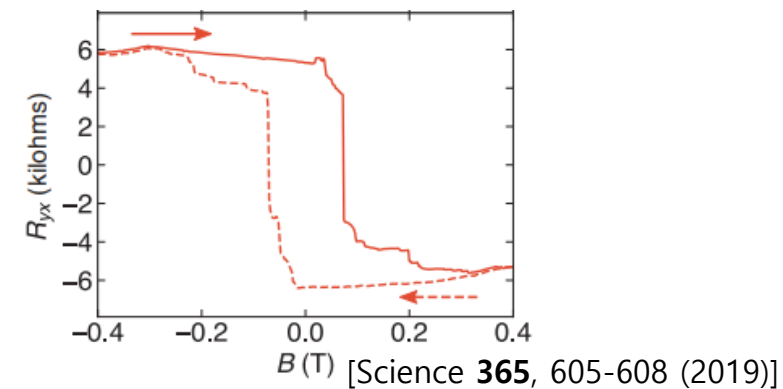
Ferroelectricity



[Nature **556**, 43 (2018)]

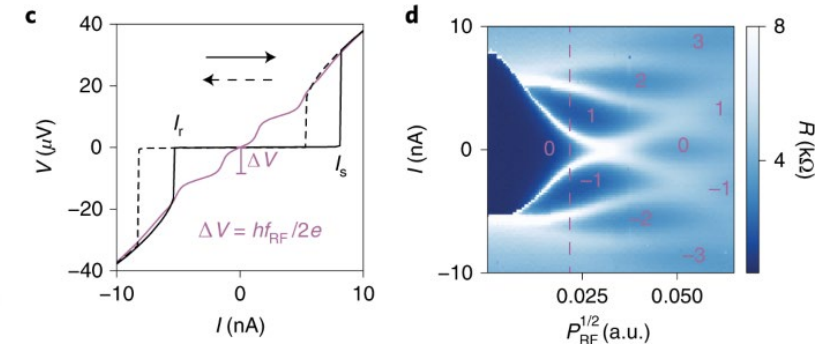
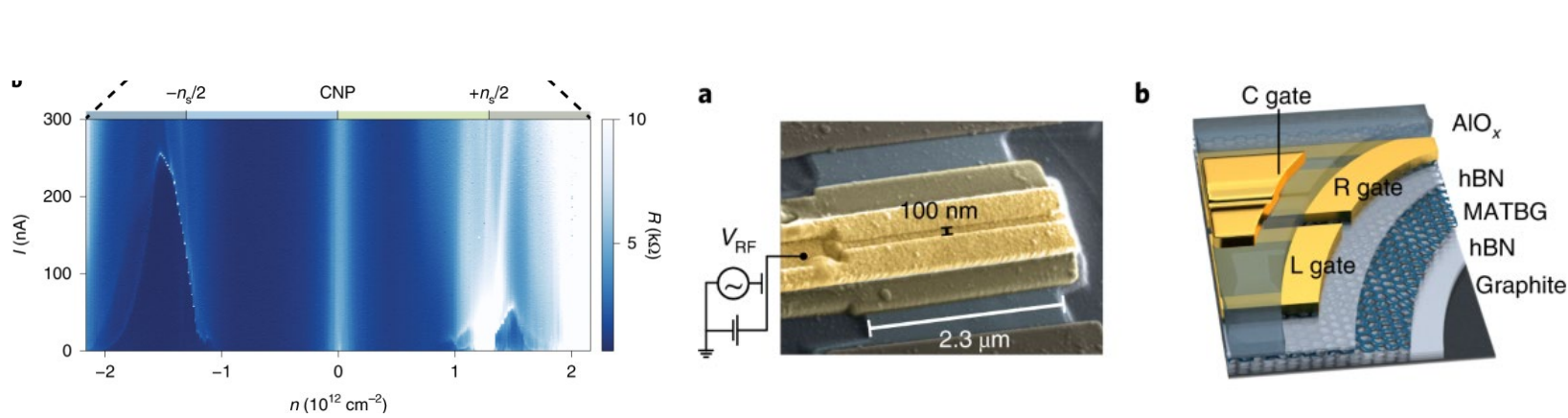
[Nature **588**, 71 (2020)]

Ferromagnetism



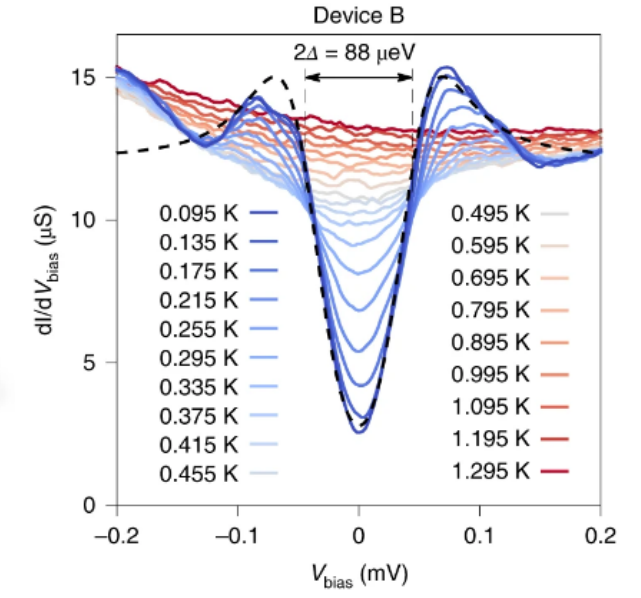
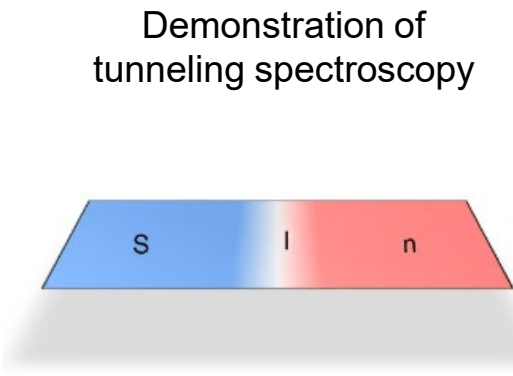
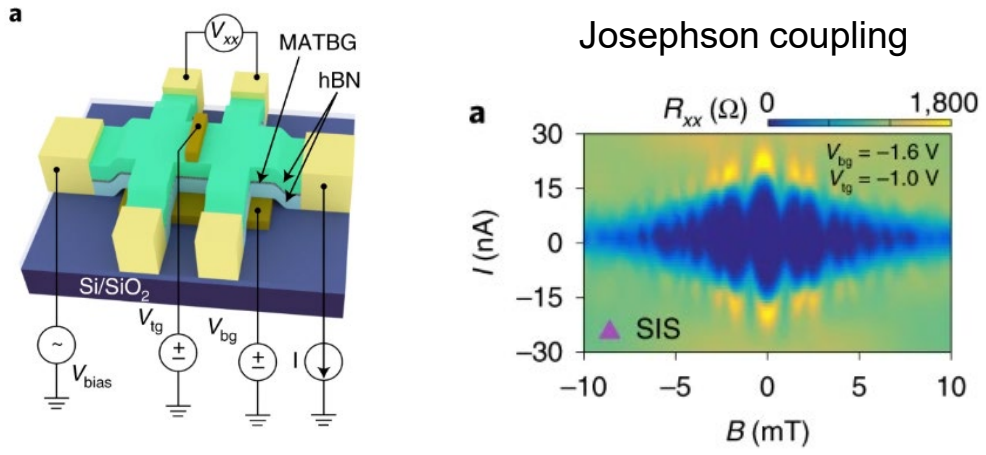
[Science **365**, 605-608 (2019)]

MATBG-based Josephson Junction



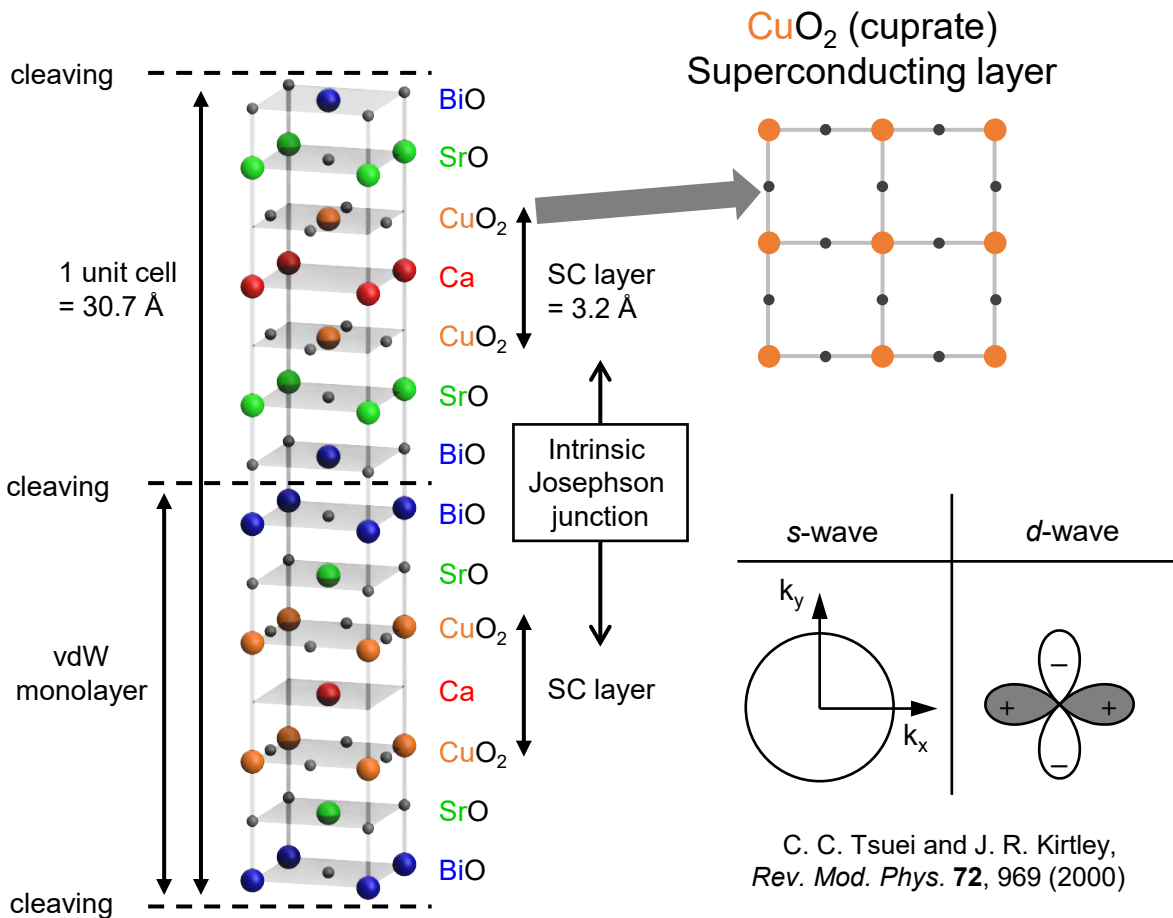
Usual Shapiro step
→ topologically trivial SC

[F. K. de Vries et al., Nat. Nanotechnol. 16, 760 (2021)]

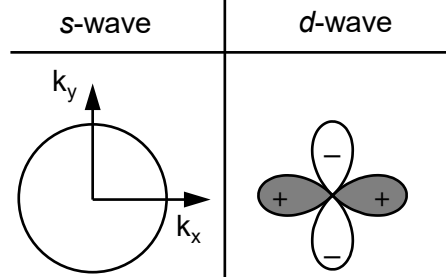
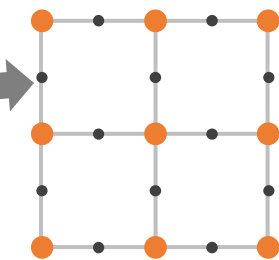


[D. Rodan-Legrain et al., Nat. Nanotechnol. 16, 769 (2021)]

Bi-2212 Twisted Josephson Junction (1/2)

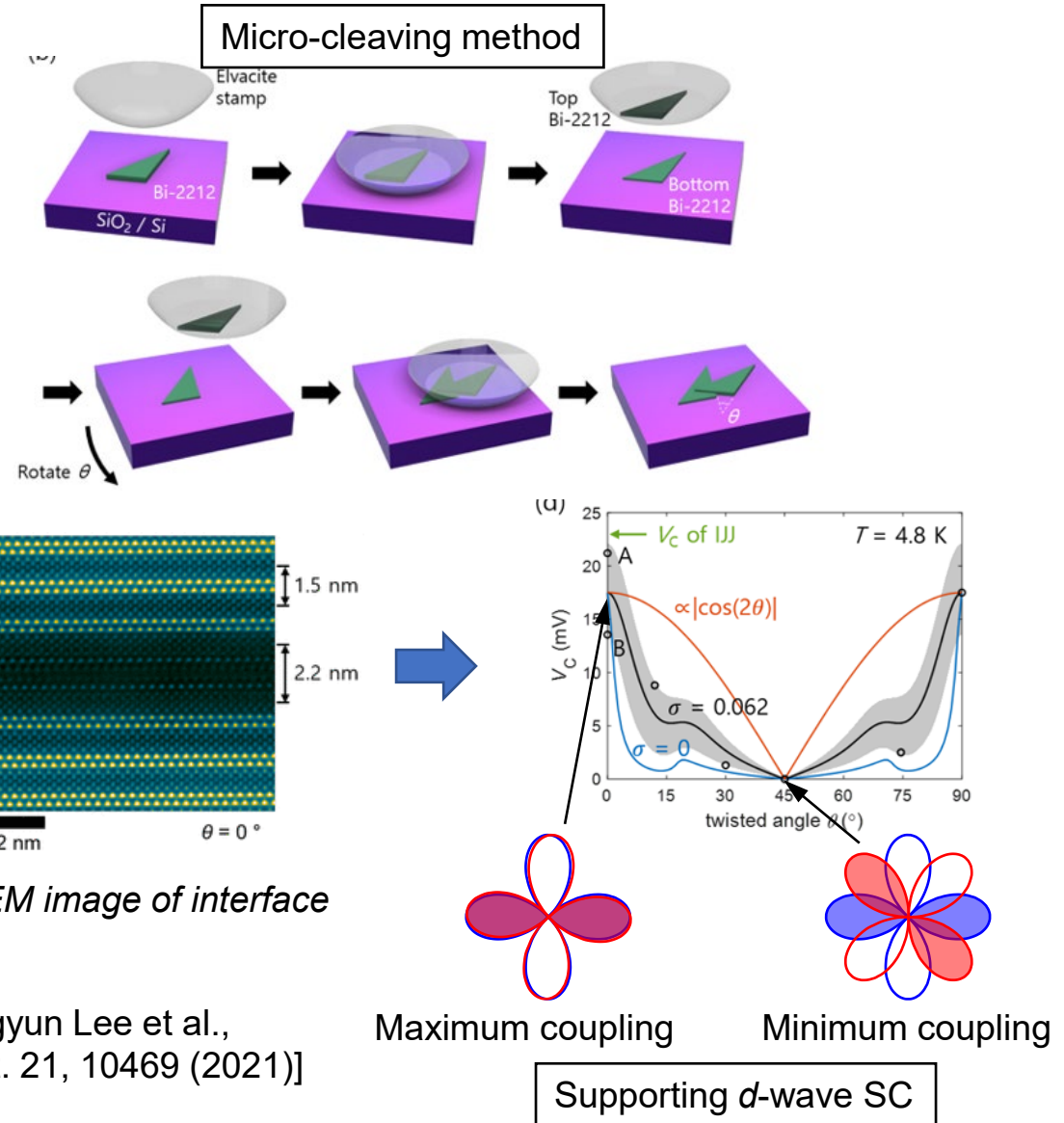


CuO₂ (cuprate)
Superconducting layer



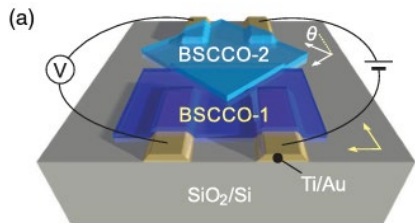
C. C. Tsuei and J. R. Kirtley,
Rev. Mod. Phys. **72**, 969 (2000)

STM, ARPES experiments shows evidences of d-wave SC

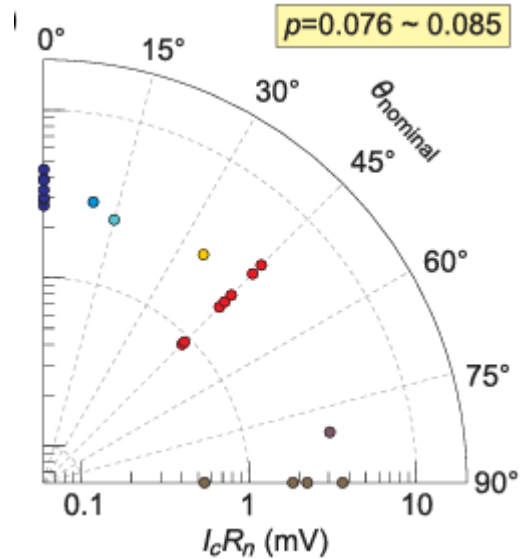
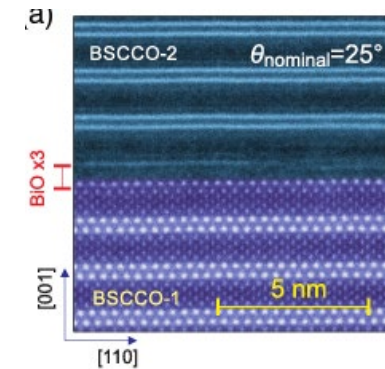
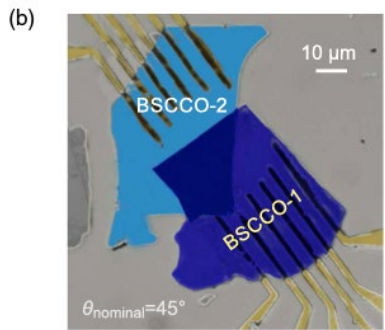


[Jongyun Lee et al.,
Nano Lett. **21**, 10469 (2021)]

Bi-2212 Twisted Josephson Junction (2/2)



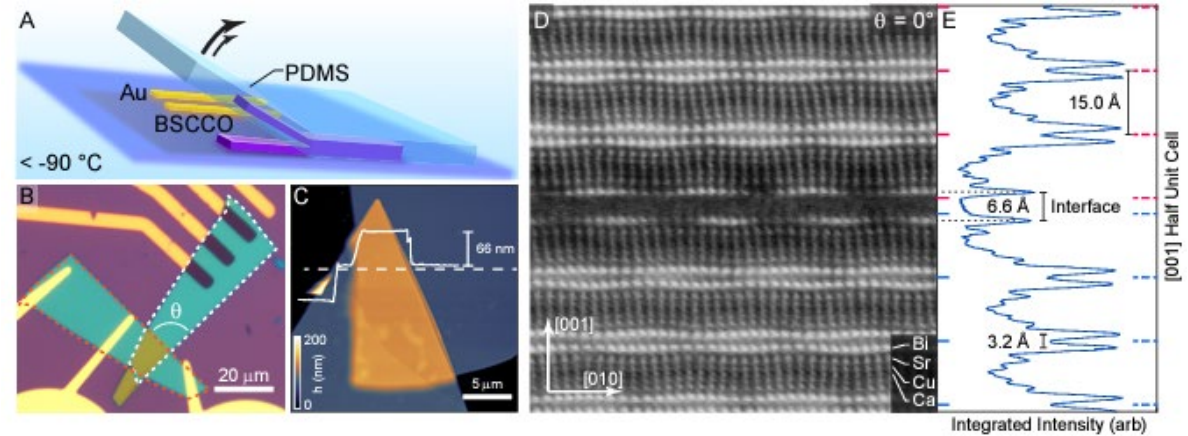
Fabricated in glovebox



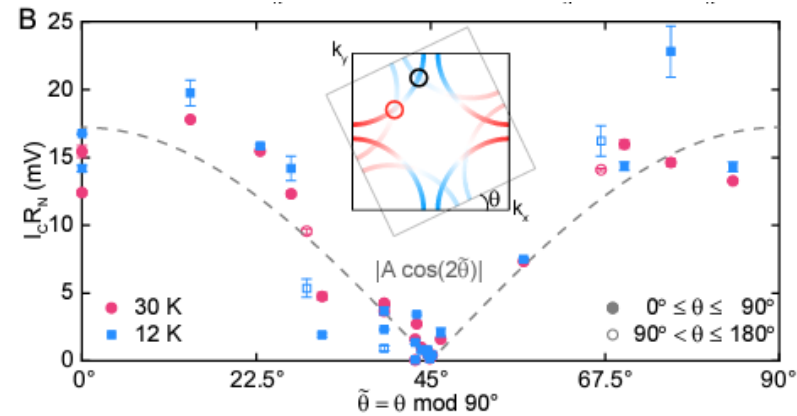
No twist-angle dependence

Supporting s-wave SC

[Y. Zhu et al., PRX 11, 031011 (2021)]



Fabricated on cold stage
in glovebox



Supporting d-wave SC

[S. Y. Frank Zhao et al., arXiv:2108.13455 (2021)]

Josephson Diode

To be updated

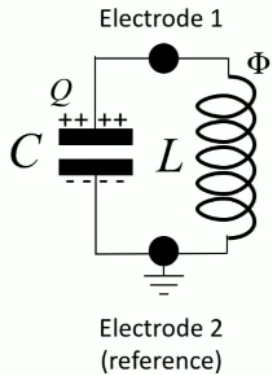
Topological Material based Josephson Junctions

To be updated

Superconducting Qubits & possible roles of vdW materials

Quantum LC Resonator

The quantized LC oscillator



Hamiltonian:

$$\hat{H}_{LC} = \frac{\hat{Q}^2}{2C} + \frac{\hat{\Phi}^2}{2L}$$

↑ Capacitive term ↑ Inductive term

Canonically conjugate variables:

$$\begin{aligned} \hat{\Phi} &= \text{Flux through the inductor.} \\ \hat{Q} &= \text{Charge on capacitor plate.} \\ [\hat{\Phi}, \hat{Q}] &= i\hbar \end{aligned}$$

M. Devoret, Les Houches Session LXIII (1995)

Correspondence with simple harmonic oscillator

$$\hat{H}_{LC} = \frac{\hat{\Phi}^2}{2L} + \frac{\hat{Q}^2}{2C}$$

$$[\hat{\Phi}, \hat{Q}] = i\hbar$$

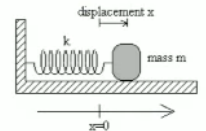
Correspondence:

$$\begin{aligned} \hat{\Phi} &\leftrightarrow \hat{X} & L &\leftrightarrow \frac{1}{k} \\ \hat{Q} &\leftrightarrow \hat{P} & C &\leftrightarrow m \end{aligned}$$

$$\hat{H}_{SHO} = \frac{k\hat{X}^2}{2} + \frac{\hat{P}^2}{2m}$$

$$[\hat{X}, \hat{P}] = i\hbar$$

$$\omega = \frac{1}{\sqrt{LC}} \leftrightarrow \sqrt{\frac{k}{m}}$$



Solve using ladder operators:

$$\hat{a} = \left(\frac{\hat{Q}}{Q_{zpf}} - i \frac{\hat{\Phi}}{\Phi_{zpf}} \right)$$

$$\Phi_{zpf} = \sqrt{2\hbar Z}$$

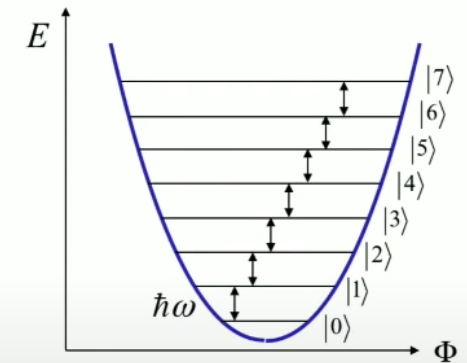
$$Q_{zpf} = \sqrt{2\hbar / Z}$$

$$\hat{a}^\dagger = \left(\frac{\hat{Q}}{Q_{zpf}} + i \frac{\hat{\Phi}}{\Phi_{zpf}} \right)$$

$$Z = \omega L = \frac{1}{\omega C} = \sqrt{\frac{L}{C}}$$

$$\hat{H}_{LC} = \hbar\omega \left(\hat{a}^\dagger \hat{a} + \frac{1}{2} \right)$$

$$[\hat{a}_r, \hat{a}_r^\dagger] = 1$$



M. Devoret, Les Houches Session LXIII (1995)

Josephson Inductance

Inductance describes voltage drop, V , induced by the change of current, dI/dt ,

$$V = L \times (dI/dt).$$

For Josephson junction,

I changes in time

→ φ changes in time (DC Josephson relationship)

→ V appears (AC Josephson relationship)

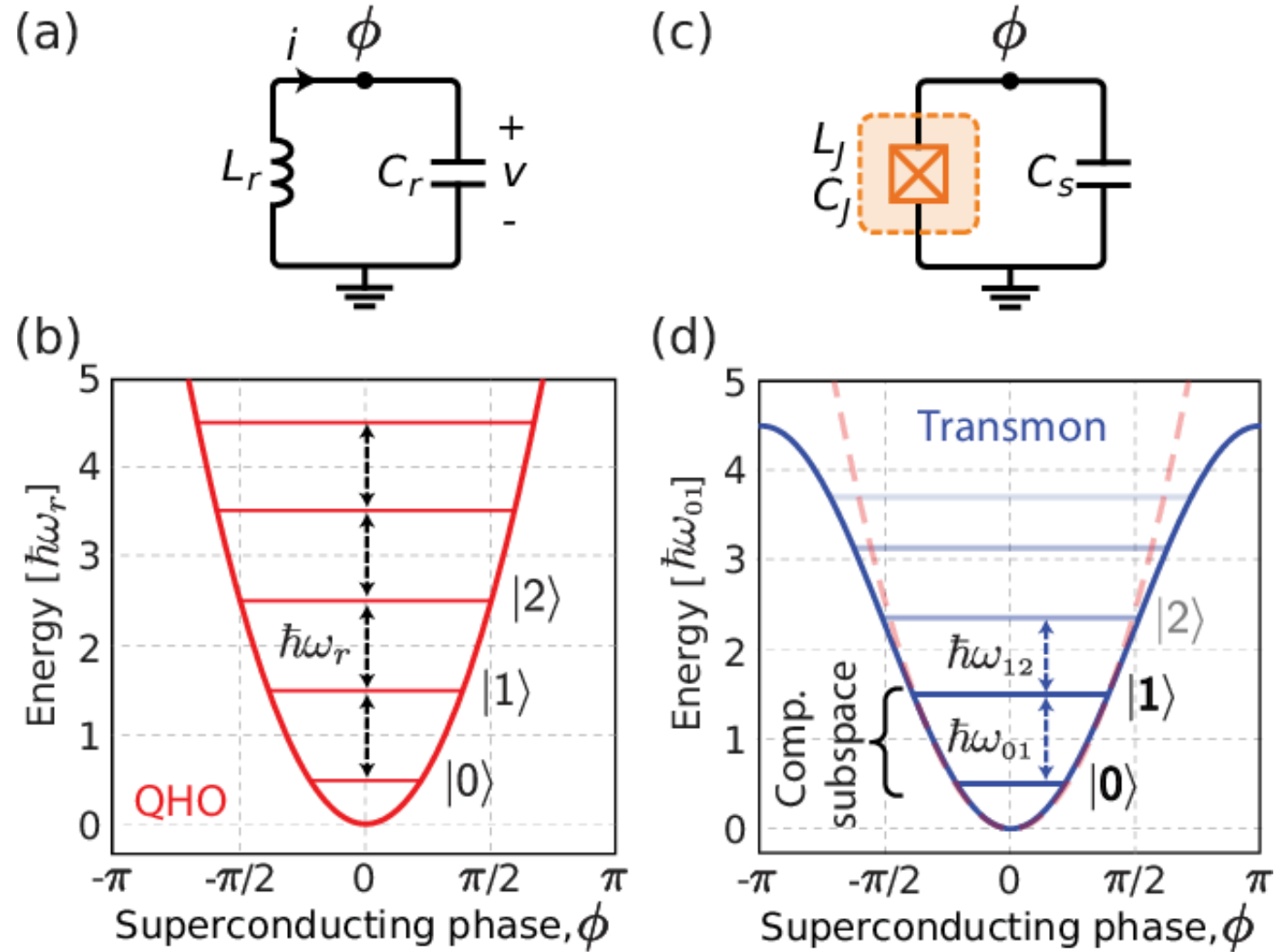
$$\begin{aligned} \frac{\partial I}{\partial \varphi} &= I_c \cos \varphi, \\ \frac{\partial \varphi}{\partial t} &= \frac{2\pi}{\Phi_0} V. \end{aligned} \longrightarrow \frac{\partial I}{\partial t} = \frac{\partial I}{\partial \varphi} \frac{\partial \varphi}{\partial t} = I_c \cos \varphi \cdot \frac{2\pi}{\Phi_0} V, \longrightarrow V = \frac{\Phi_0}{2\pi I_c \cos \varphi} \frac{\partial I}{\partial t} = \boxed{L(\varphi)} \frac{\partial I}{\partial t}.$$

Josephson inductance

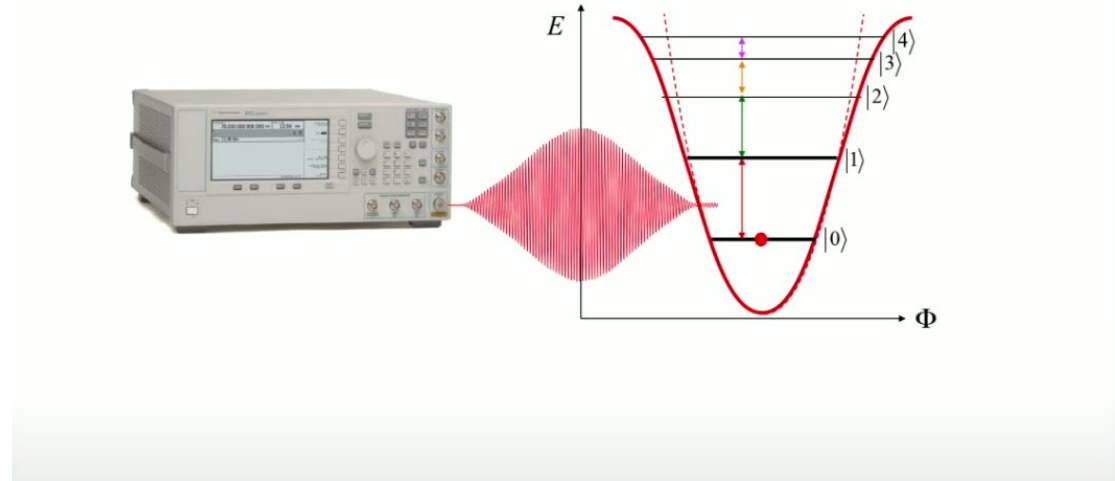
$$L(\varphi) = \frac{\Phi_0}{2\pi I_c \cos \varphi} = \frac{L_J}{\cos \varphi}. \quad L_J = L(0) = \frac{\Phi_0}{2\pi I_c}$$

Josephson junction is a 'quantum' nonlinear inductor.

Anharmonic LC resonator



Transmon energy spectrum

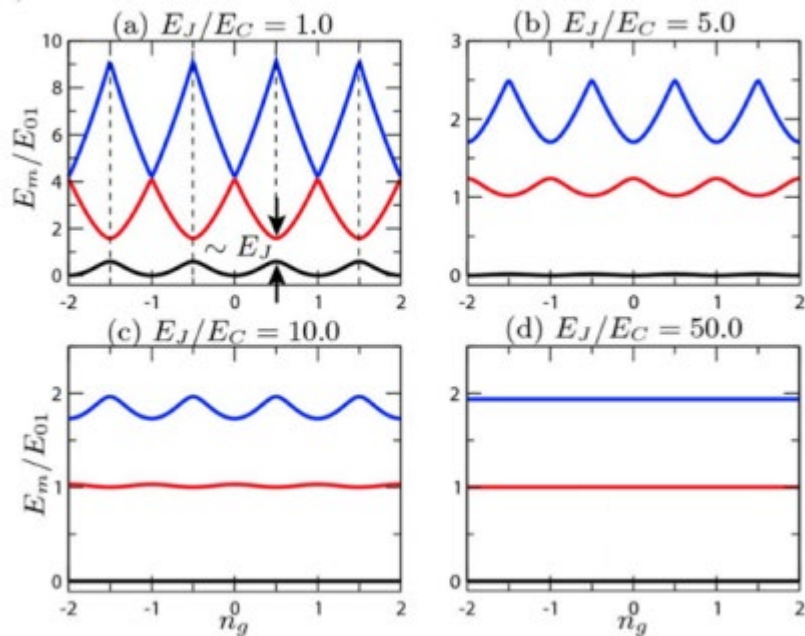


Shunting Capacitor

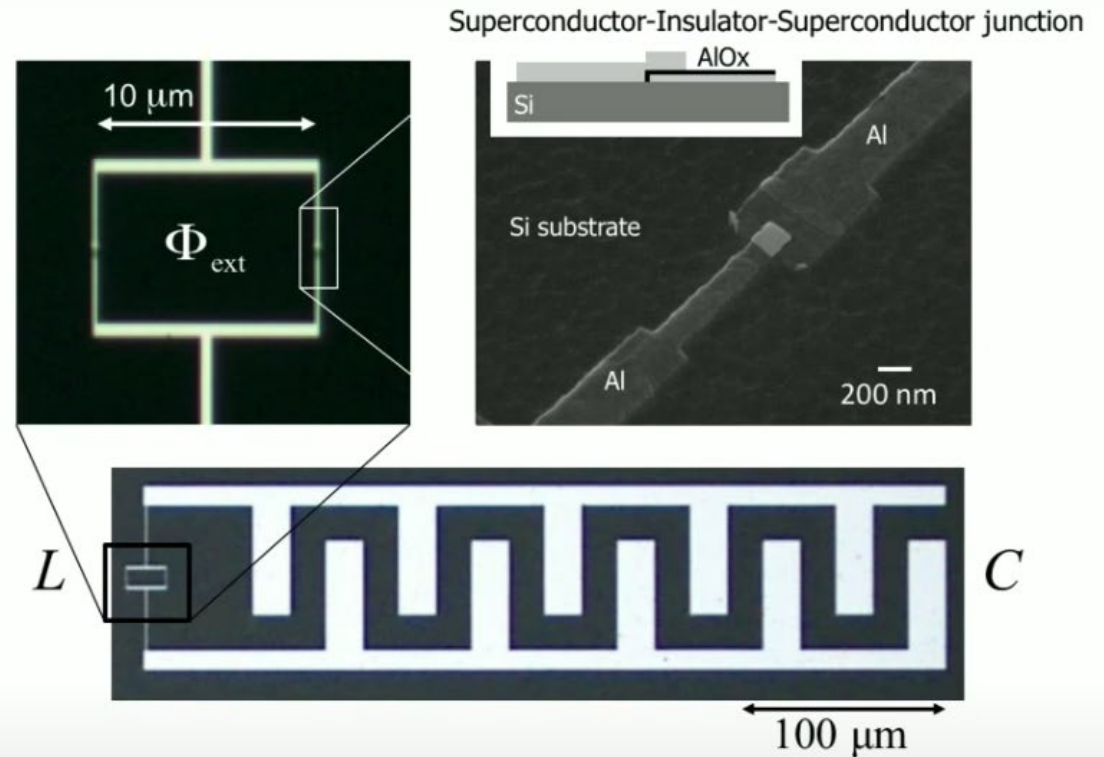
$$\text{Energy stored in } C: E = \frac{(ne)^2}{2C} = E_C n^2$$

To minimize effect charge noise, E_C was decreased by adding big capacitor.

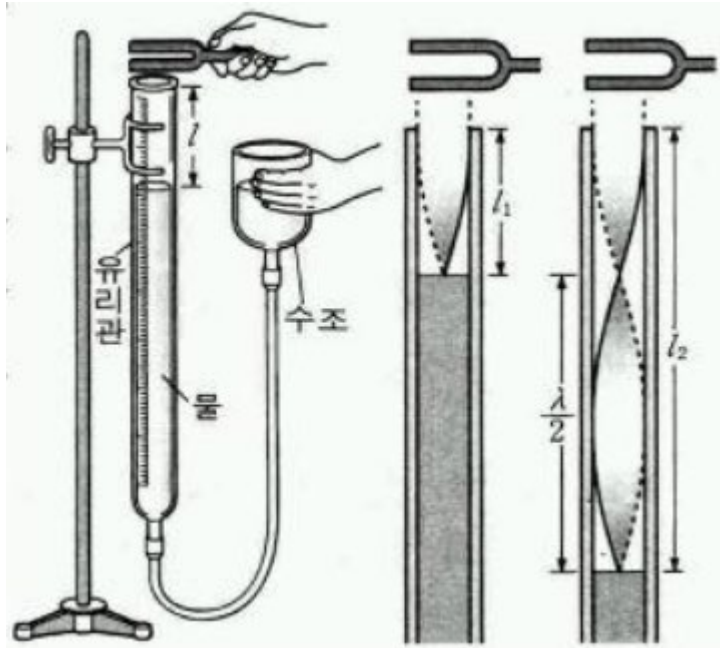
Energy diagram as a function of charging



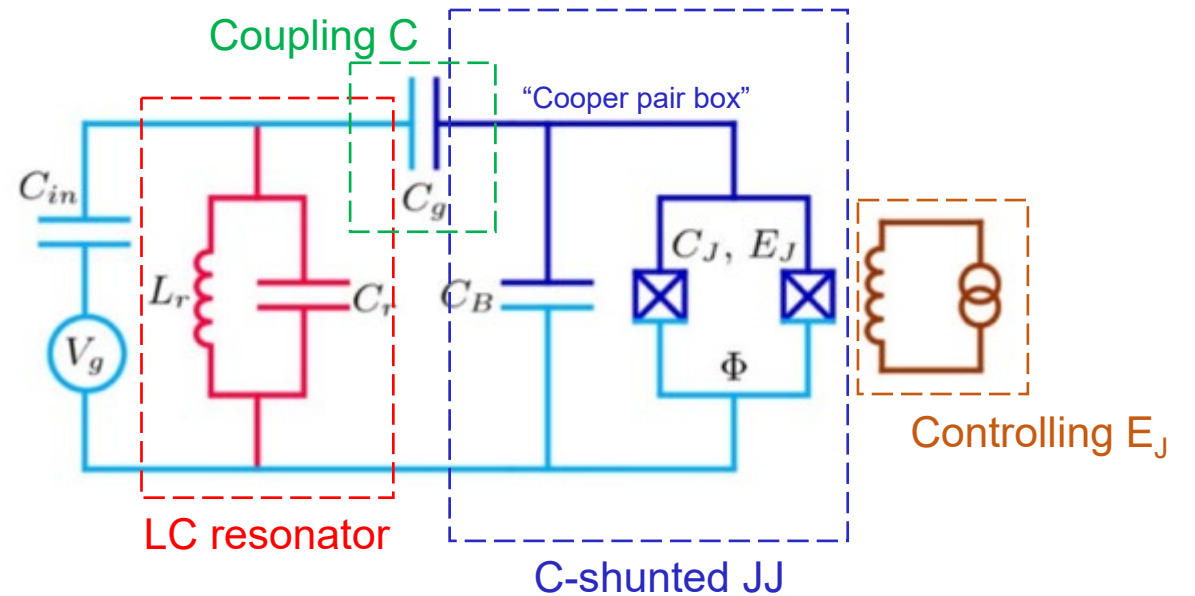
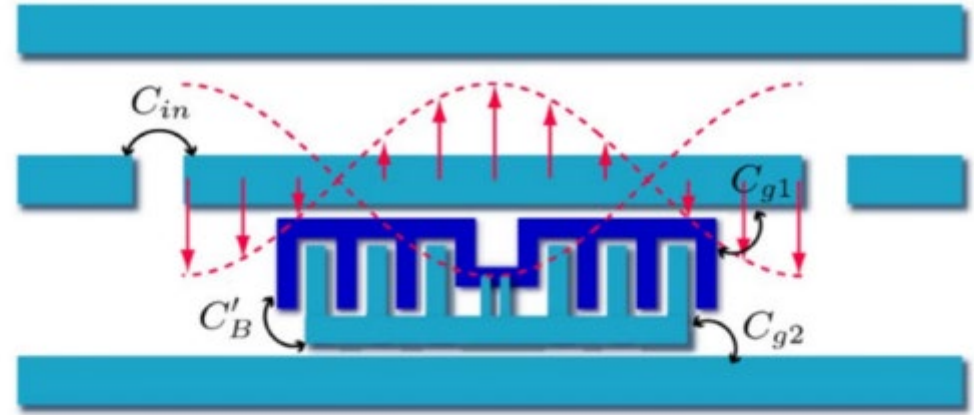
Two-junction transmon



Coplanar Waveguide (CPW) coupled to Transmon

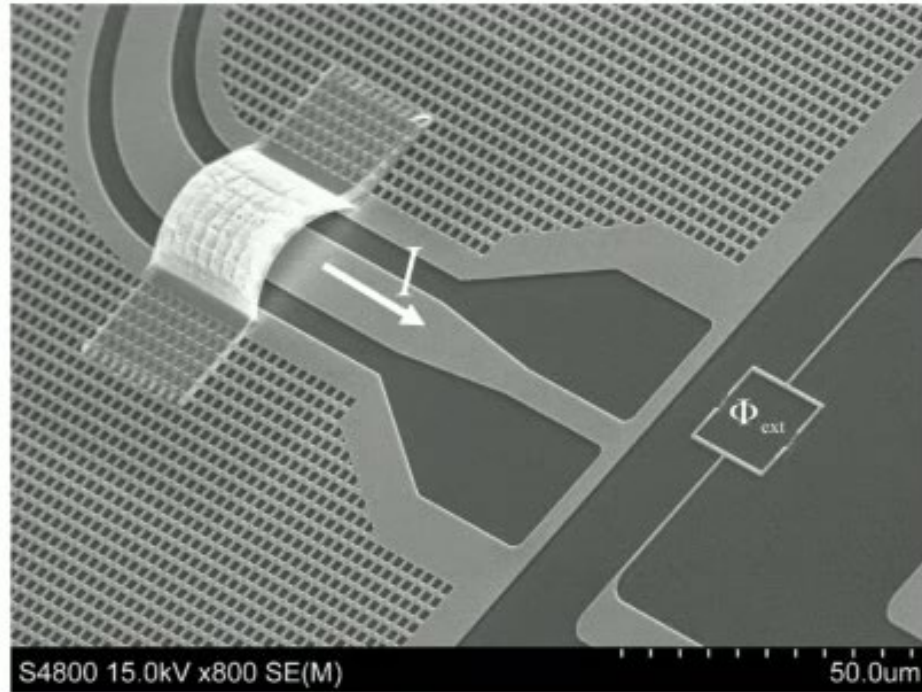


Air Column Resonance
(기주공명)

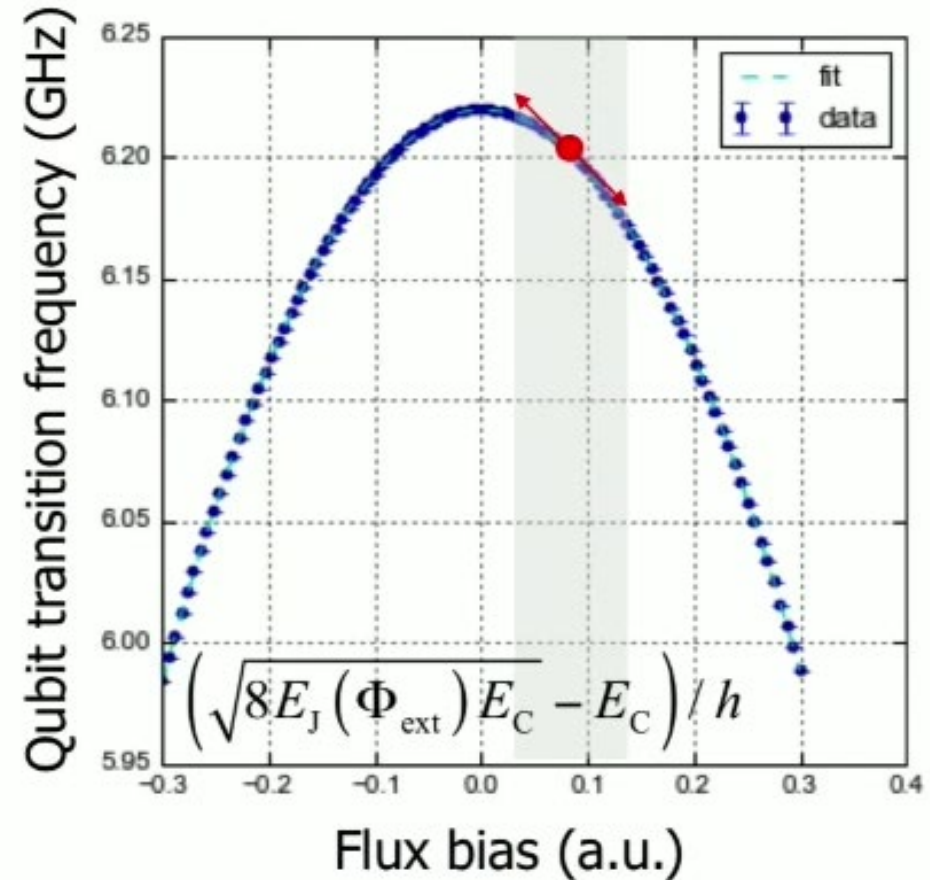


Flux control of Transmon Frequency

Short-circuited transmission line

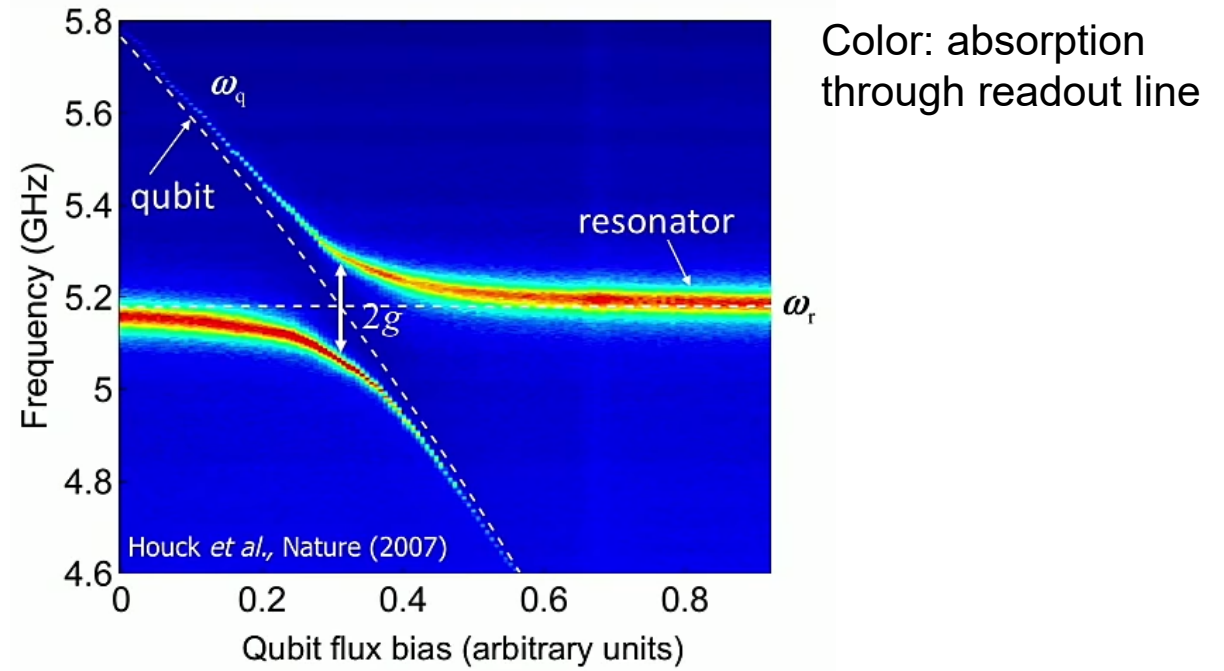
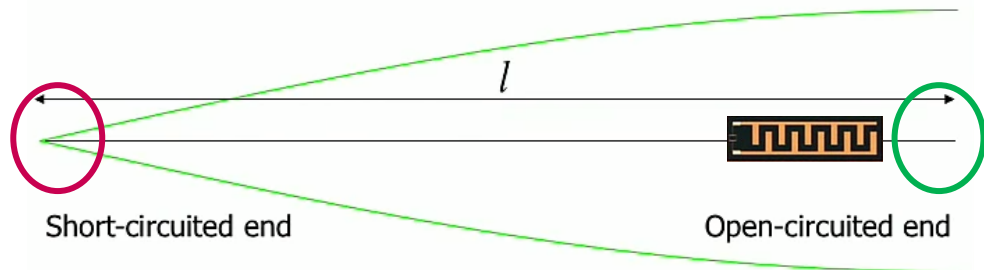
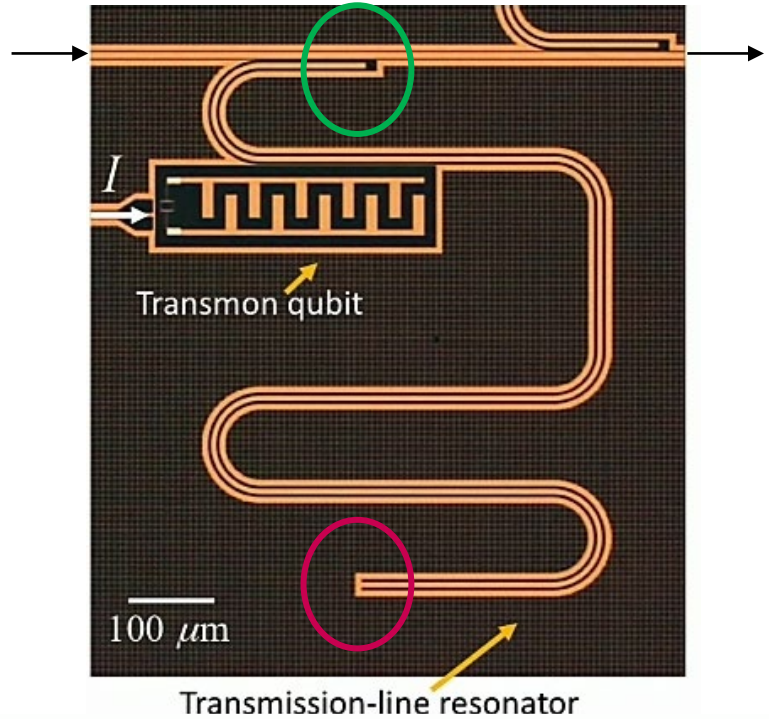


$$L_J = L(0) = \frac{\Phi_0}{2\pi I_c} \quad \rightarrow \quad \omega = \frac{1}{\sqrt{LC}}$$



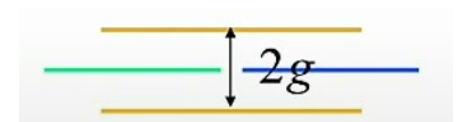
Qubit-Resonator Interaction

Qubit and resonator are capacitively coupled.

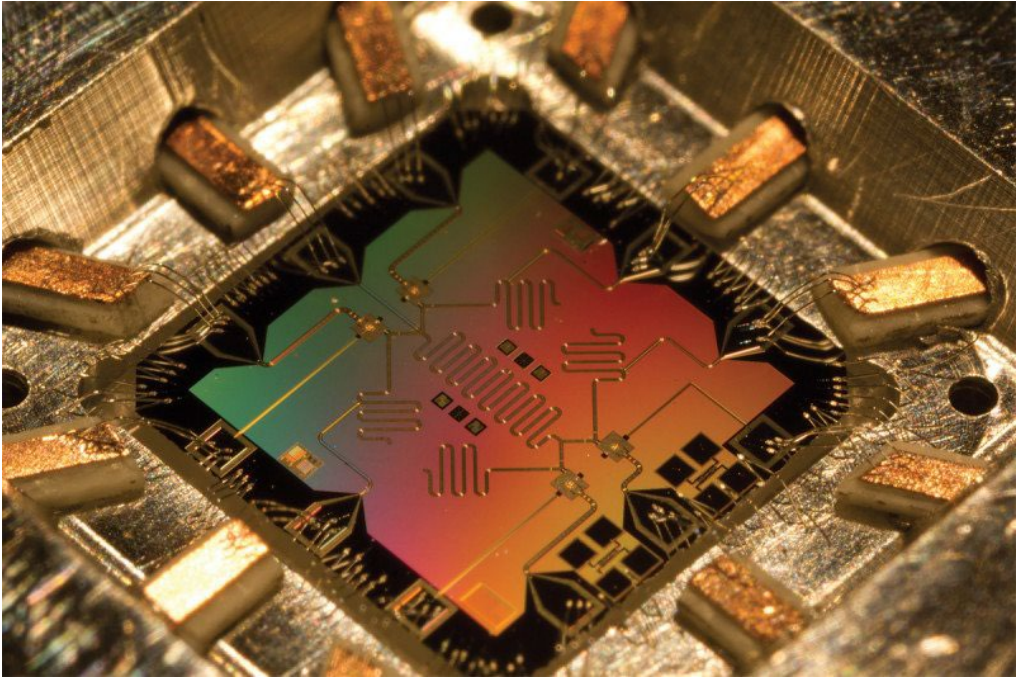
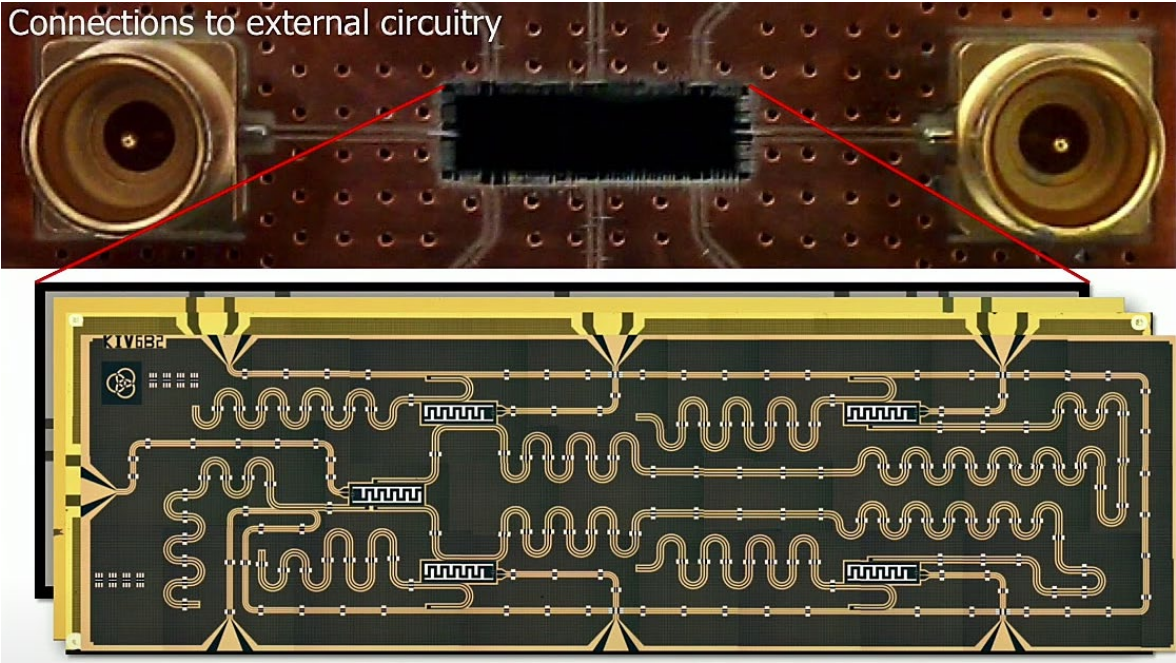


$$\hat{H}_{\text{int}} = \hbar g (a_r \hat{\sigma}_+ + a_r^\dagger \hat{\sigma}_-) \quad \text{Jaynes-Cummings interaction}$$

Decrease qubit state
Increase resonator state

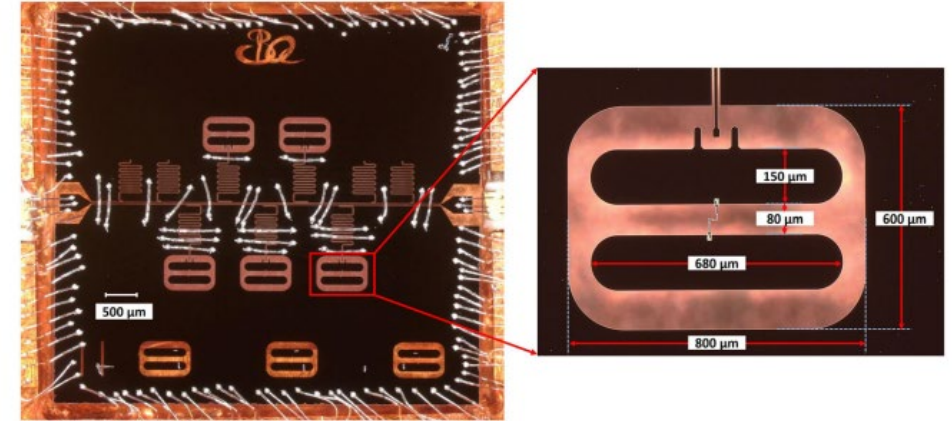
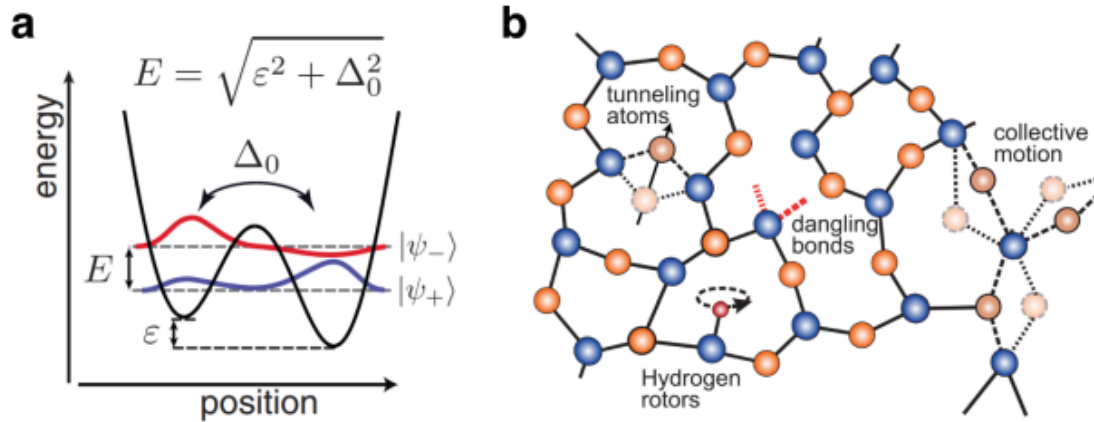


Connections to External Circuitry



Google version

Two Level System & State-of-art Transmon Qubit



Transmon qubit made with α -Ta film on Sapphire substrate

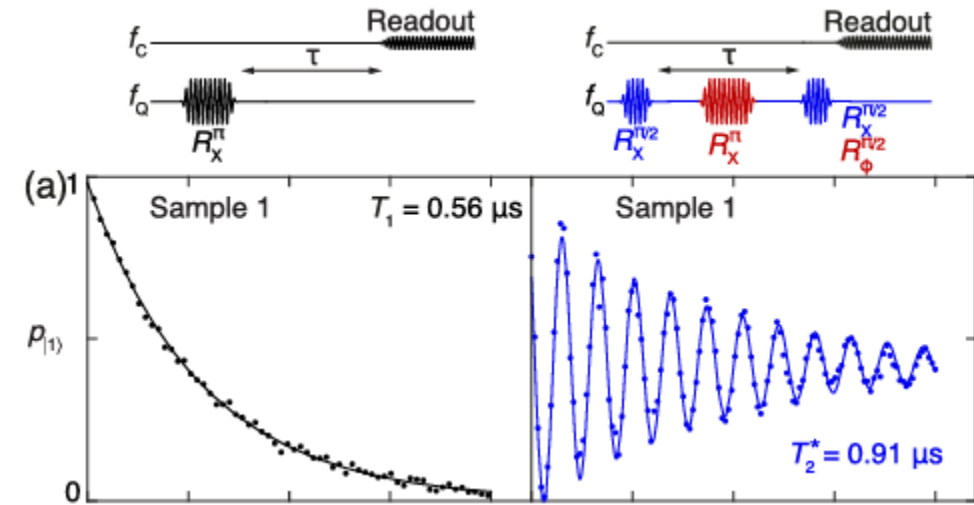
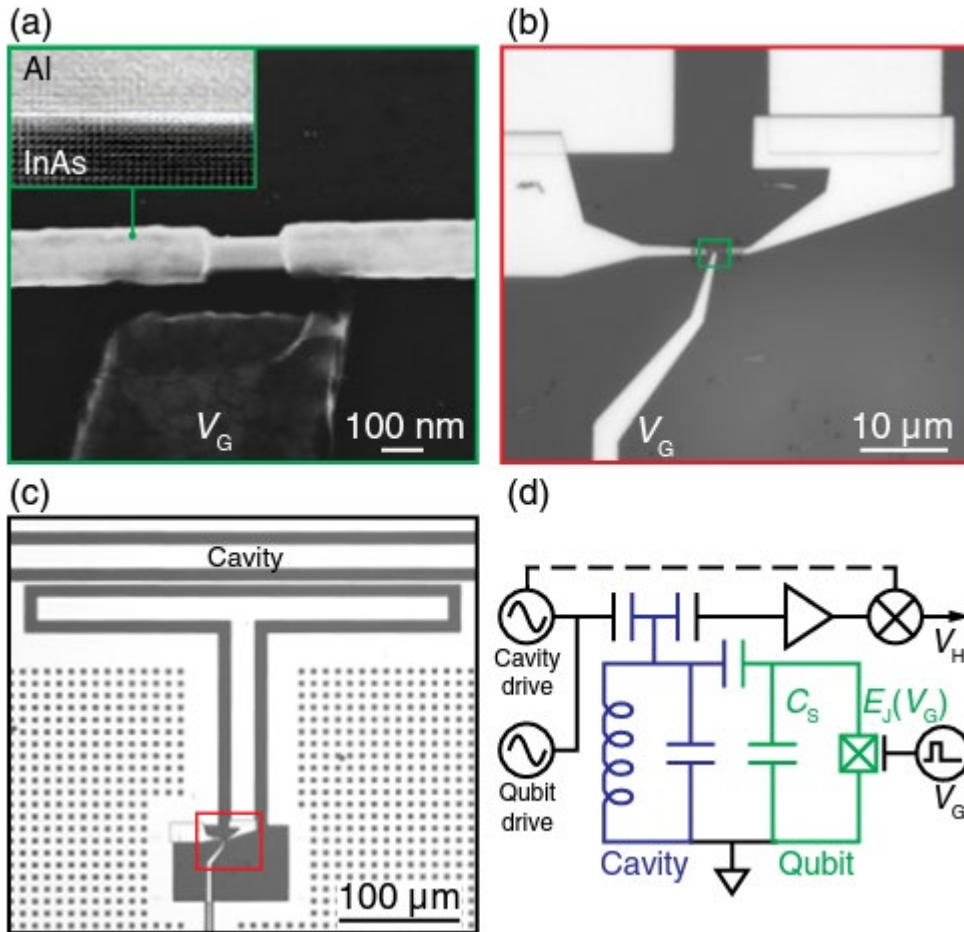
- Energy relaxation time $T_1 \sim 500 \mu\text{s}$

Applications of van der Waals Materials for Superconducting Quantum Devices
[A. Antony, PhD Thesis]

[A.P. M. Place et al., Nat. Comm. 12, 1779 (2021)]
[C. Wang et al., npj Quantum Information 8, 3 (2022)]

Al/InAs/Al Gatemon Qubit

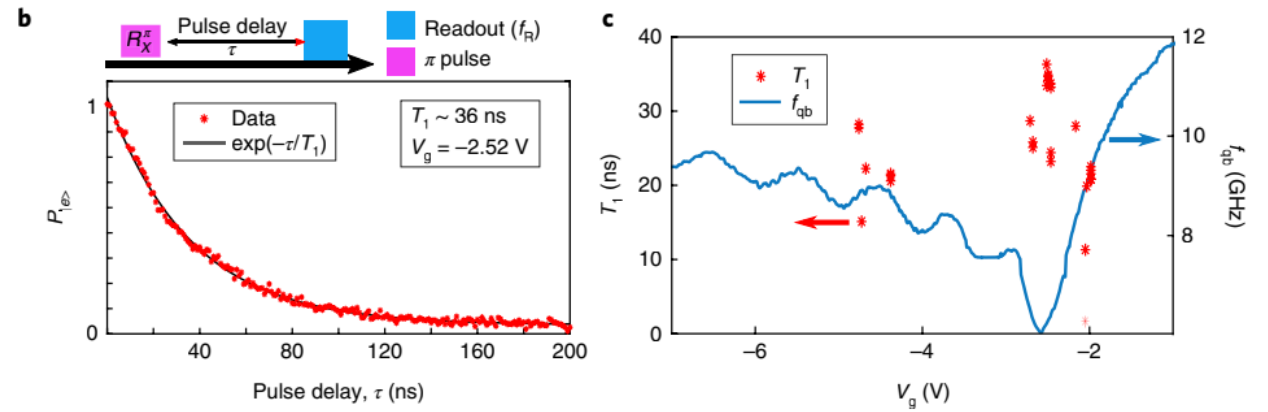
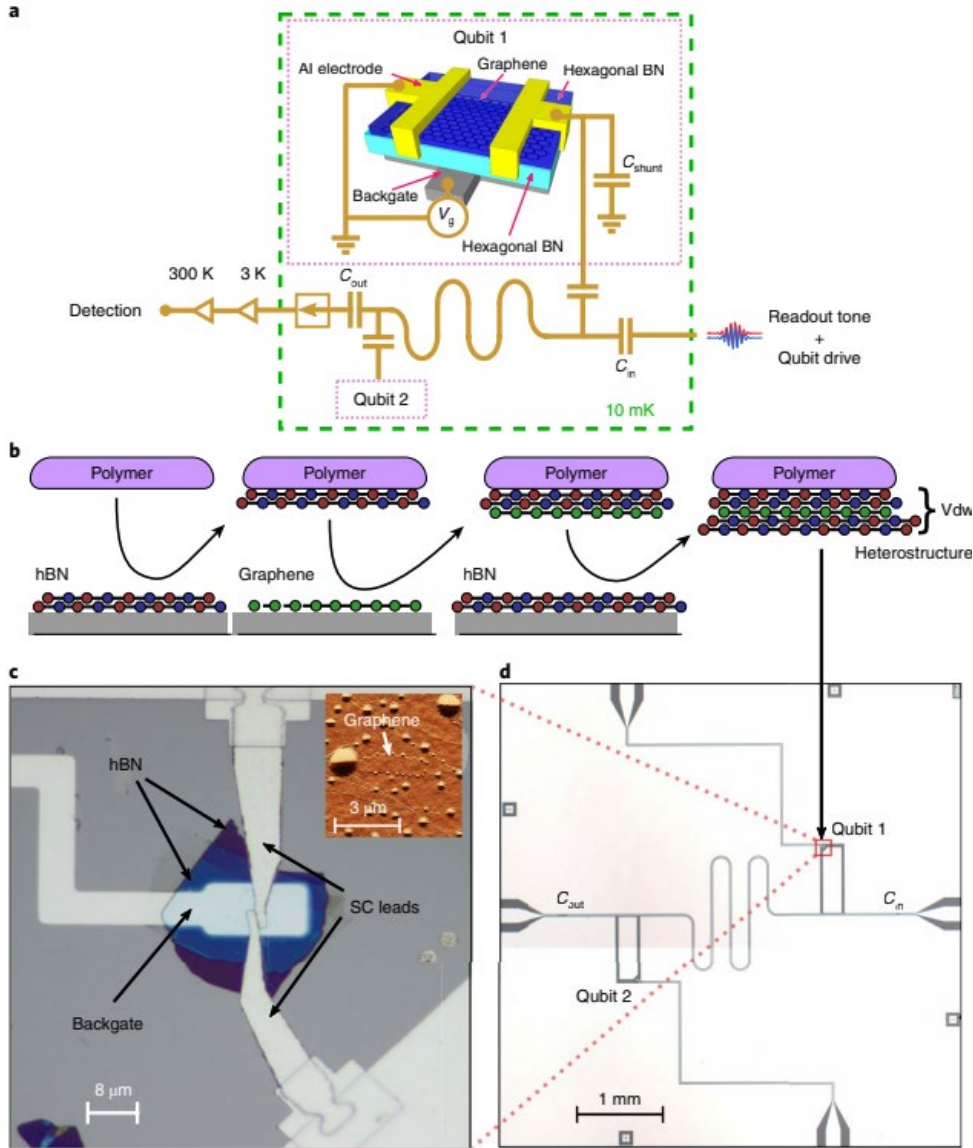
Al is epitaxially grown on InAs nanowire.



- Energy relaxation time $T_1 \sim 0.8 \mu\text{s}$
- Dephasing time $T_2^* \sim 1 \mu\text{s}$

Semiconductor-Nanowire-Based Superconducting Qubit
 [T. W. Larsen et al., PRL 115, 127001 (2015)]

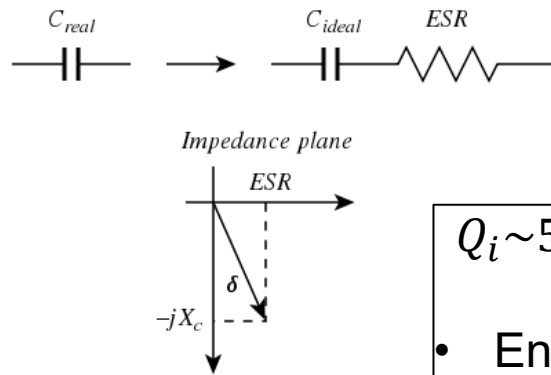
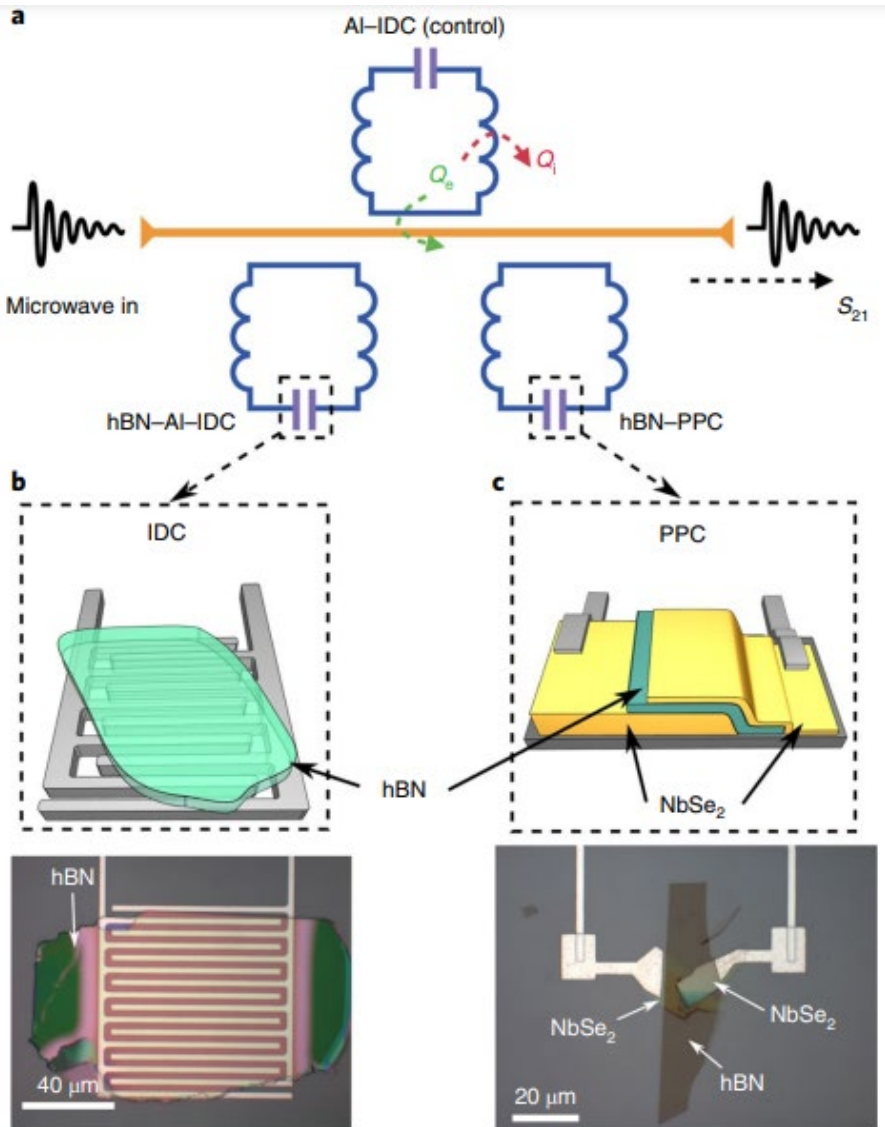
Graphene-based Gatemon Qubit



- Energy relaxation time $T_1 \sim 30 \text{ ns}$
- Dephasing time $T_2^* \sim 50 \text{ ns}$

Coherent control of a hybrid superconducting circuit made with graphene-based van der Waals heterostructures
 [J. I. Wang et al., Nat. Nanotechnol. 14, 120-125 (2019)]

hBN-based Capacitor for Transmon Qubit (1/2)



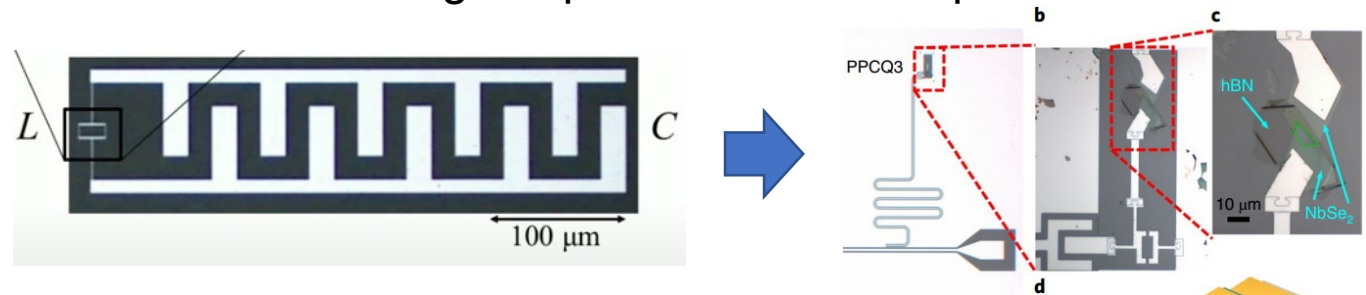
Loss tangent δ describes the loss in capacitor.

$$Q_i = 1/\tan\delta$$

$Q_i \sim 5 \times 10^6$ in a single photon limit.

- Energy relaxation time $T_1 \sim 25 \mu\text{s}$
- Dephasing time $T_2^* \sim 25 \mu\text{s}$

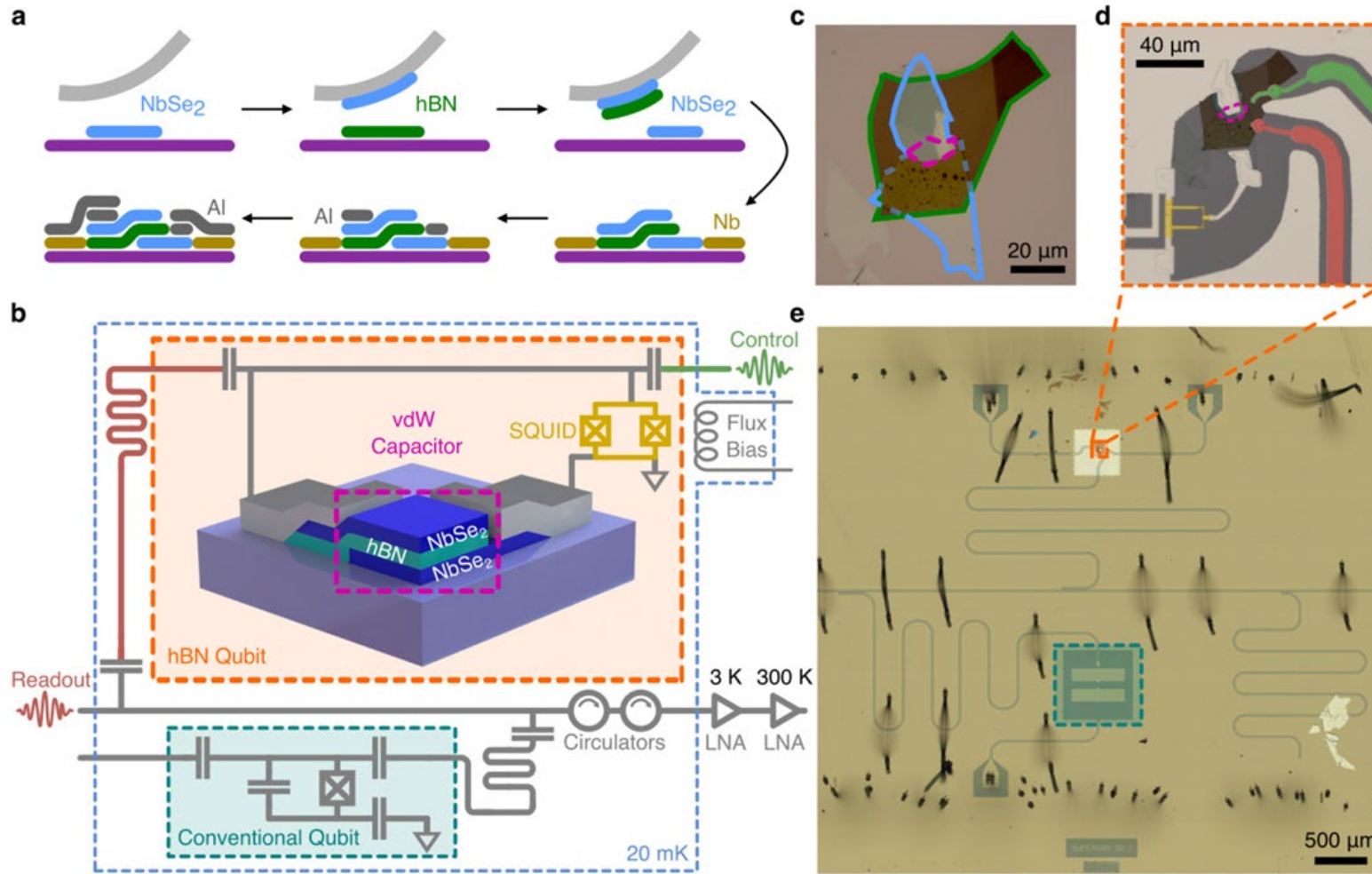
Reducing footprint of transmon qubit



Hexagonal boron nitride as a low-loss dielectric for superconducting quantum circuits and qubits

[J. I. Wang et al., Nat. Mater. 21, 398-403 (2022)]

hBN-based Capacitor for Transmon Qubit (2/2)



- Energy relaxation time $T_1 \sim 1.1 \mu s$
- Dephasing time $T_2^* \sim 1.7 \mu s$

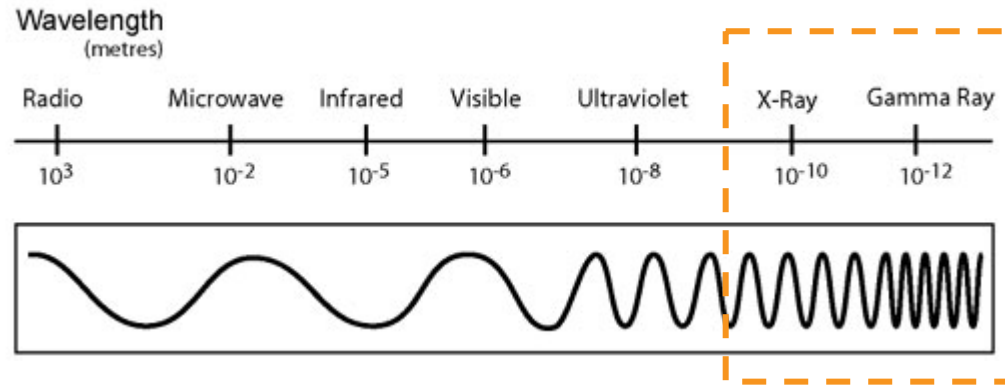
Reducing footprint of transmon qubit by 1,000 times

Miniaturizing Transmon Qubits Using van der Waals Materials
 [A. Antony et al., Nano Lett. 21, 10122 (2021)]

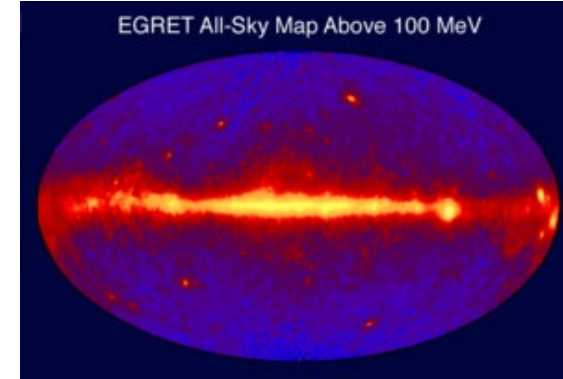
Superconducting Sensor

Ref: Superconducting photon detectors, doi.org/10.1080/00107514.2022.2043596

X/ γ -Ray



Medical X-ray imaging



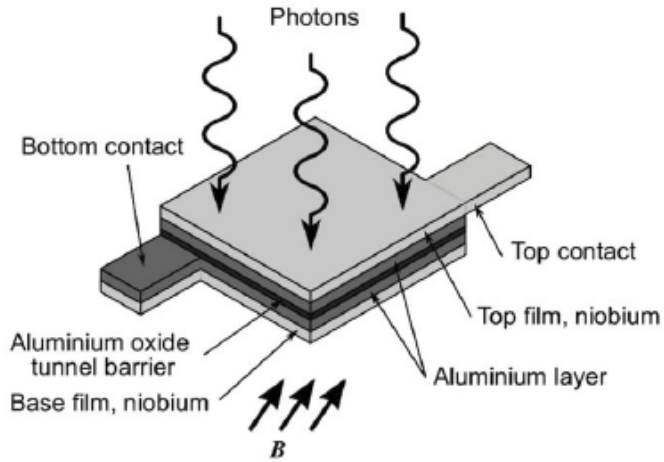
Gamma ray sky

- in **X/ γ -ray** range
 - Medical imaging
 - Material science
 - Astronomy science

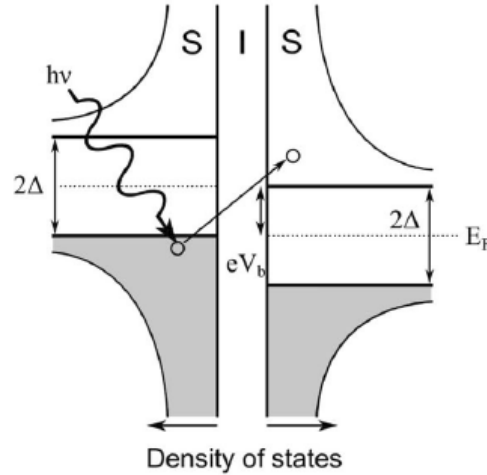


Material Science using synchrotrons

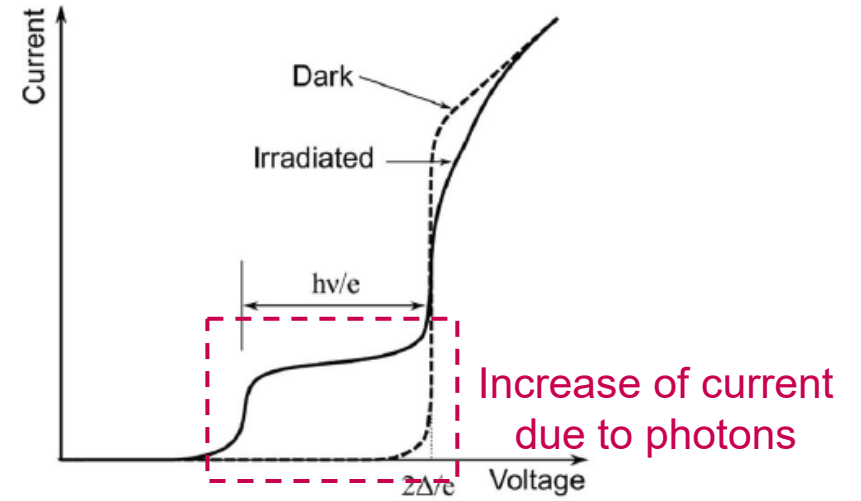
Superconducting Tunnel Junction (STJ)



In-plane magnetic field B suppresses supercurrent.



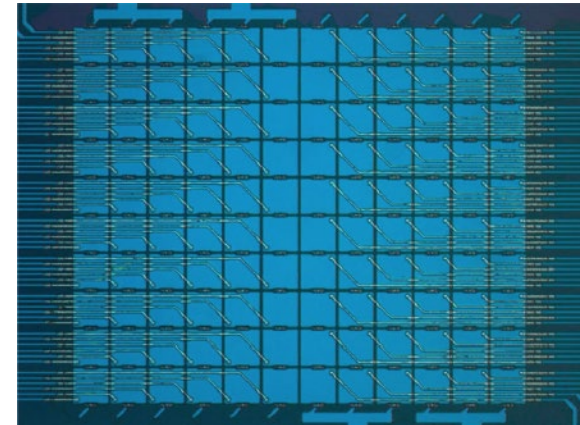
2Δ : Cooper pair binding energy



[Energy resolution]
 (photon energy)
 \propto (# of created quasi-particle)
 \propto (resulting current pulse)

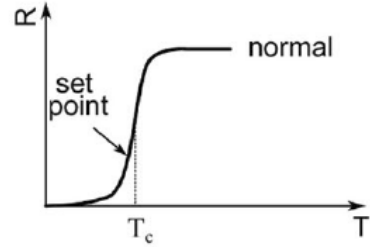
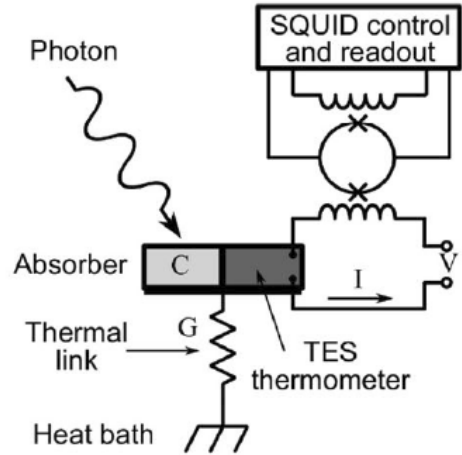
STJ covers Visible ~ UV ~ X-ray

Array of STJ



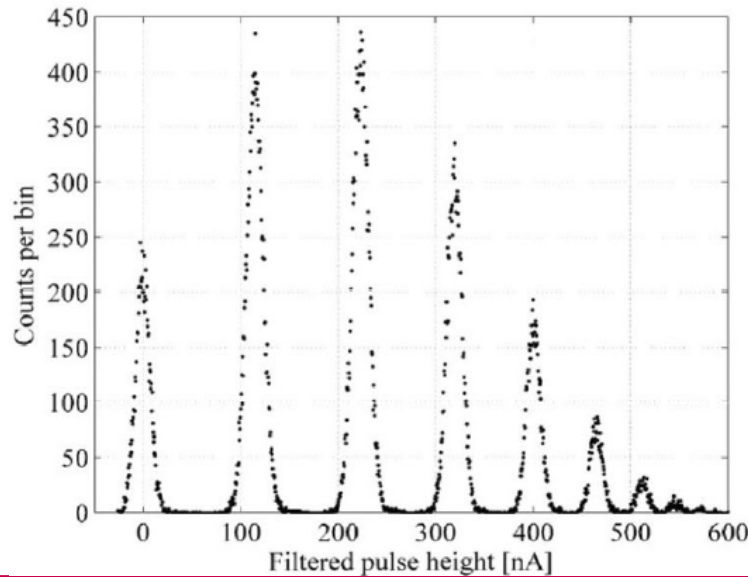
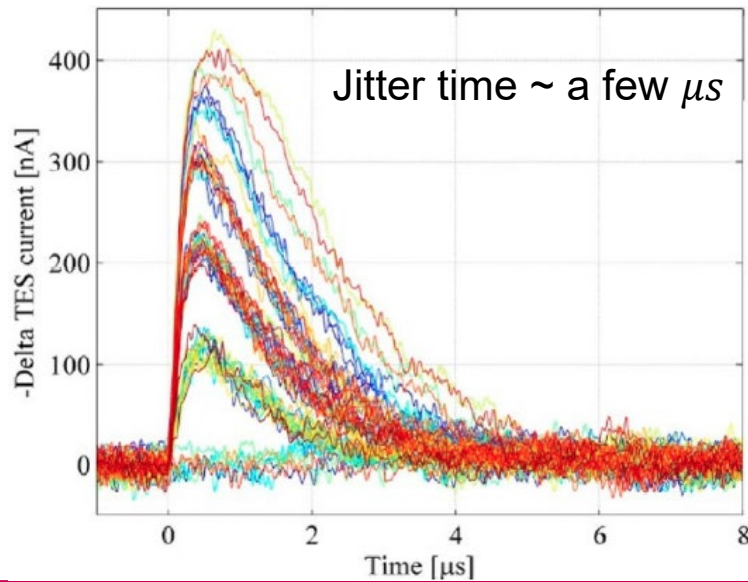
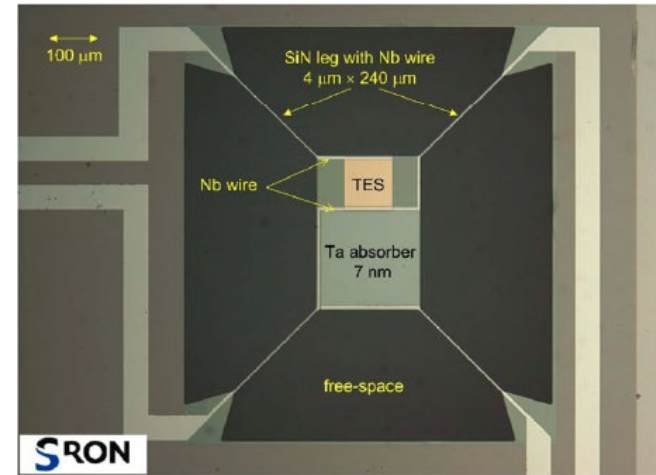
[Proc SPIE vol 6269 p. 238–248 (2006)]

Transition Edge Sensor (TES)



[Operation principle]

- Photon is absorbed
- Heats up SC
- resistance changes
- current changes (voltage-biased)
- Measured by SQUID

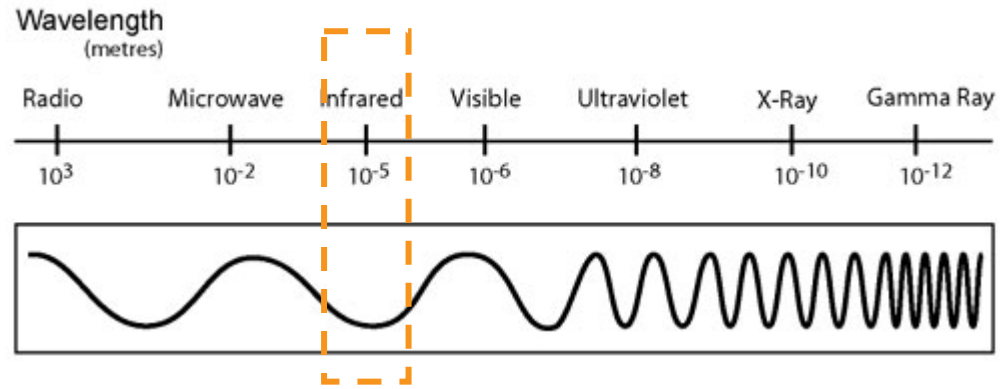


TES covers THz ~ X-ray

[Photon number resolving]
(Photon number)
 \propto (Height of current pulse)

[Proc SPIE 7681, 71–80 (2010)]
[IEEE Trans. Appl. Supercond. 21, 188–191 (2011)]

Infra-red

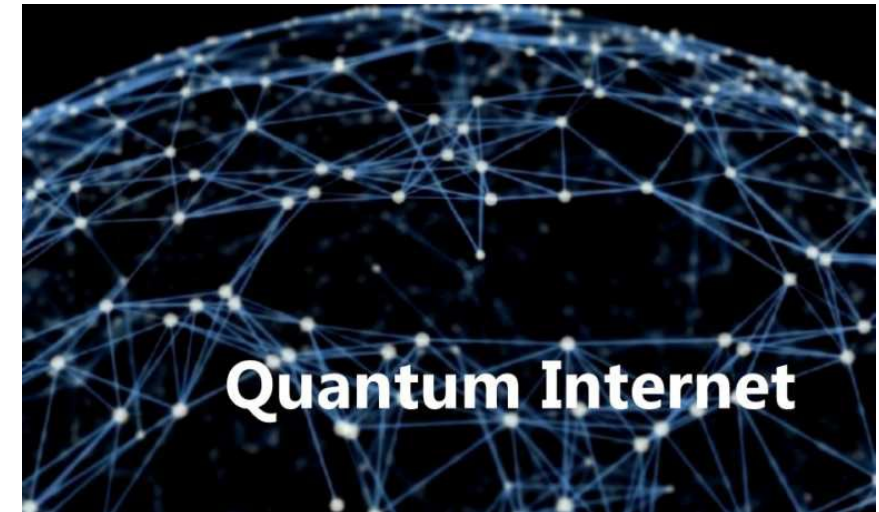


Infrared camera

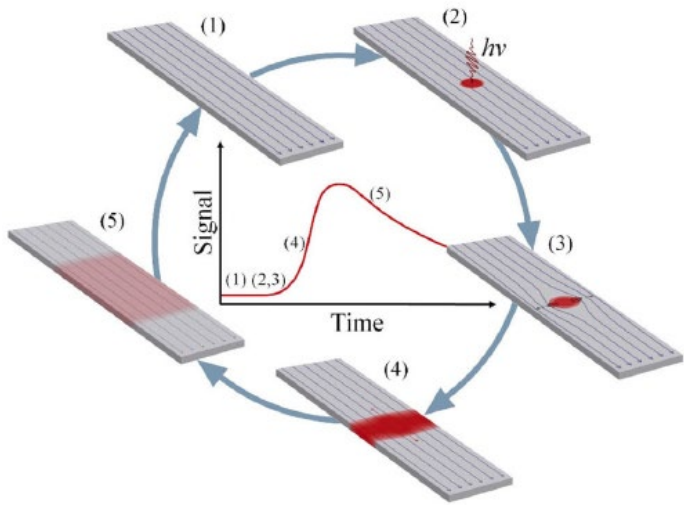


Optical cable

- in **IR** range
 - optical quantum communication
 - quantum key distribution



Superconducting Nanowire Single Photon Detector (SNSPD)



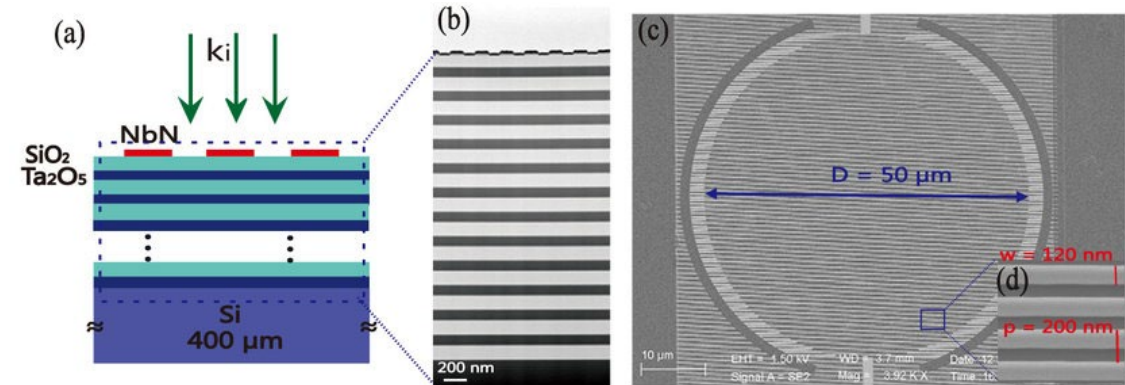
[Operation principle]

Current biased (I_b) right below I_c
→ Photon is absorbed
→ Heats up SC
→ I_b exceeds I_c
→ Generates voltage pulse

Jitter time ~ a few ps

- SNSPD is widely used for
 - long-distance quantum key distribution in optical fiber
 - quantum networks with remotely entangled qubits
 - receivers for space-to-ground classical communications
 - NASA Deep Space Optical Communications (DSOC) mission
 - scalable platform for optical quantum computing
 - optical neuromorphic computing
 - low mass/energy Dark Matter searches

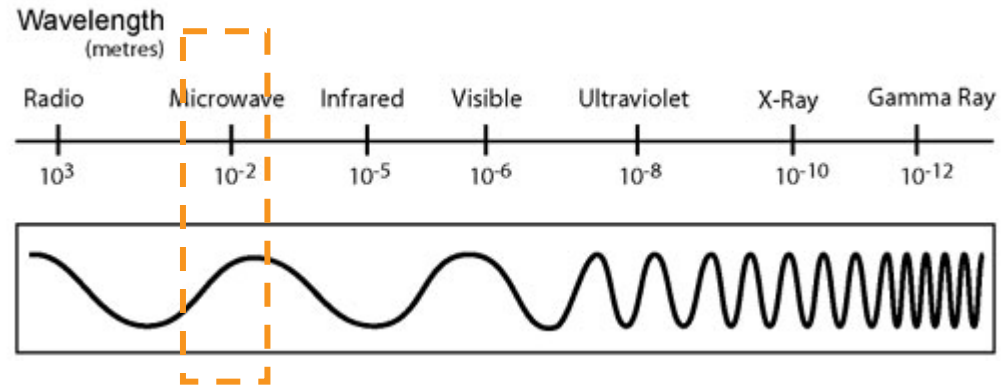
SNSPD embedded in optical cavity



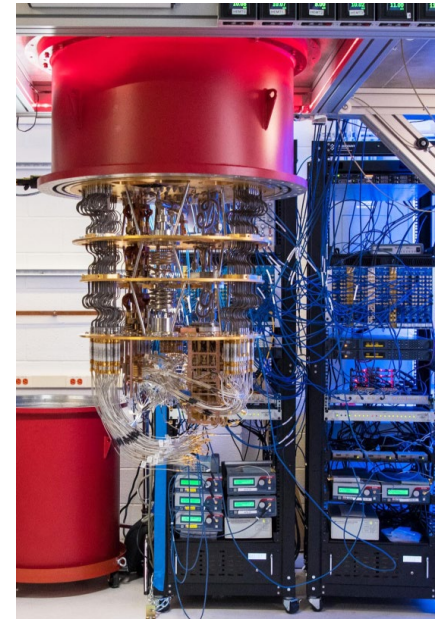
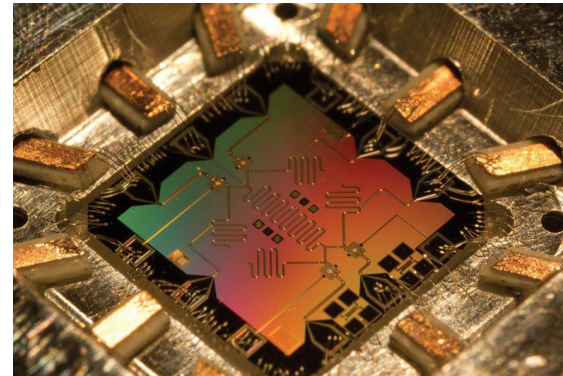
[Opt. Exp. 23, 17301-17308 (2015)]

- Various SCs are used depending on purpose. e.g.) NbN, NbTiN, TaN, MoN, WSi, MoSi, MgB₂, YBCO, BSCCO, NbSe₂, etc.

Microwave



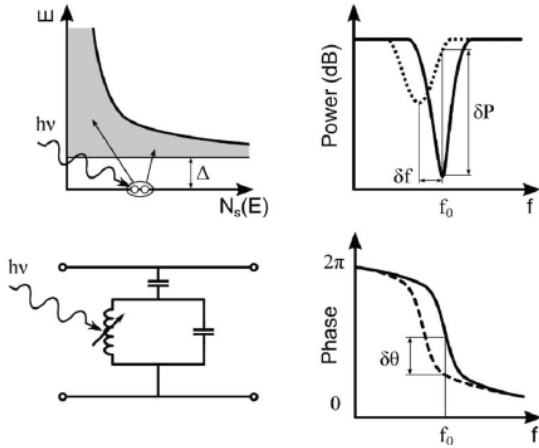
- in **GHz** range
 - remote entanglement of superconducting qubits
 - high-fidelity quantum measurements
 - microwave quantum illumination



Microwave Kinetic Inductance Detector (MKID)

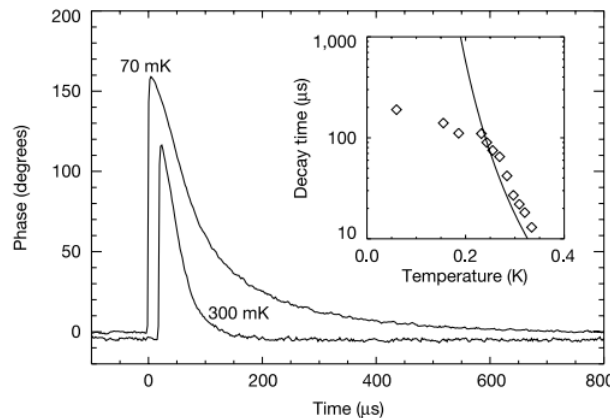
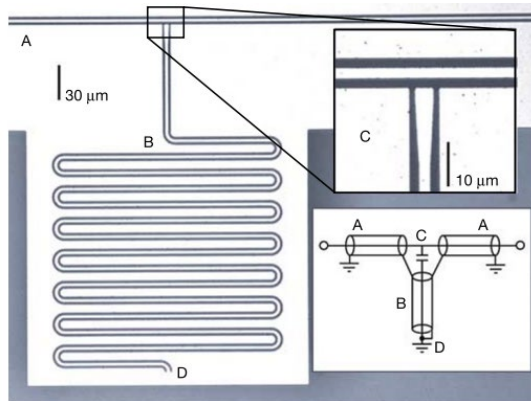
Kinetic inductance is due to inertial mass of charge carrier in AC electric field.

$$F = m \times (dv/dt) \quad \longleftrightarrow \quad V = L_K \times (dI/dt) \quad L_K = \frac{m_e l}{2n_s e^2 A}$$



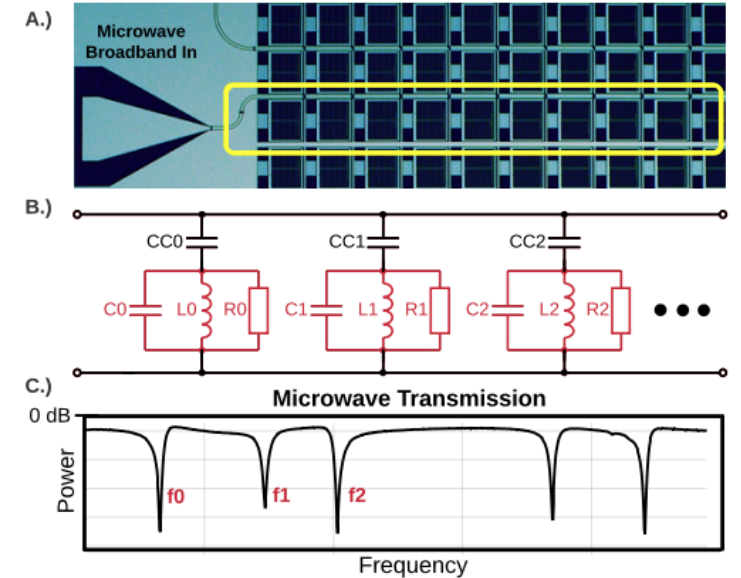
[Operation principle]

- Photon is absorbed
- L_K changes
- Resonance frequency changes
- Detect via transmitted microwave



[Nature 425, 817–821 (2003)]

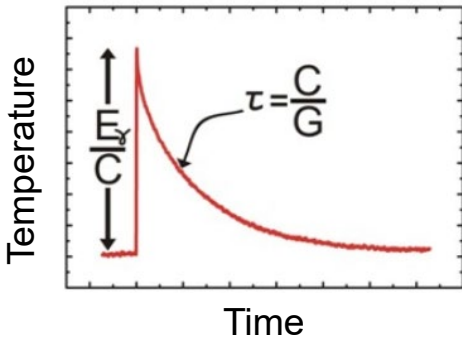
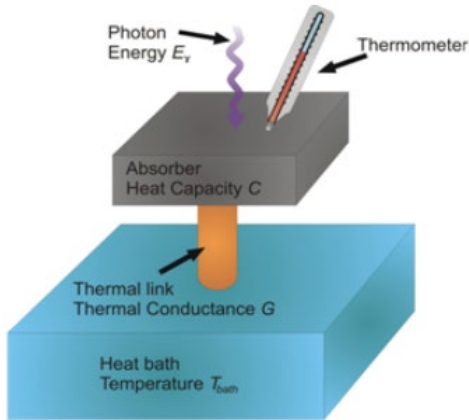
Multiplexing for imaging



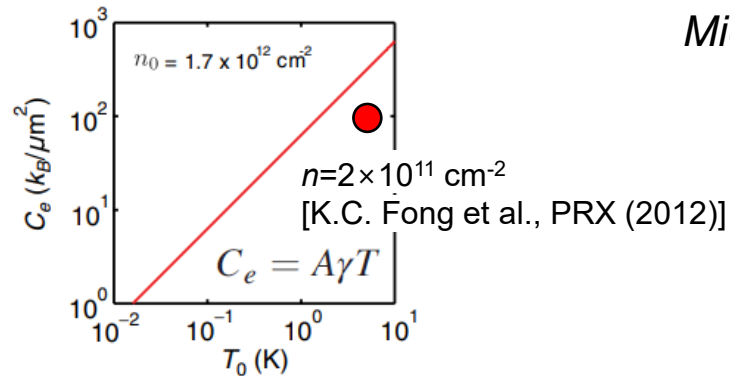
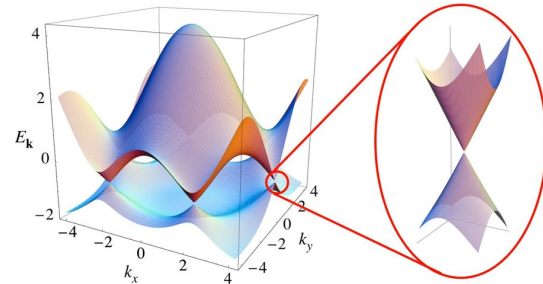
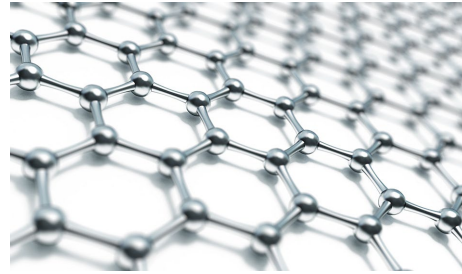
[arXiv:2203.16520v1 (2022)]

Graphene-based Josephson Junction Bolometer/SPD

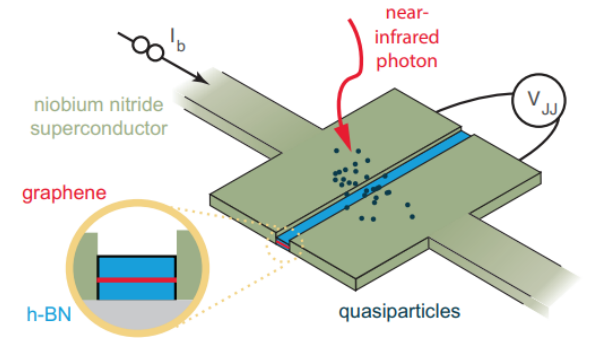
Exploit graphene's *extremely small electronic heat capacity* for detecting microwave photons



E_γ : Photon energy
 C : Heat capacity
 G : Thermal conductance

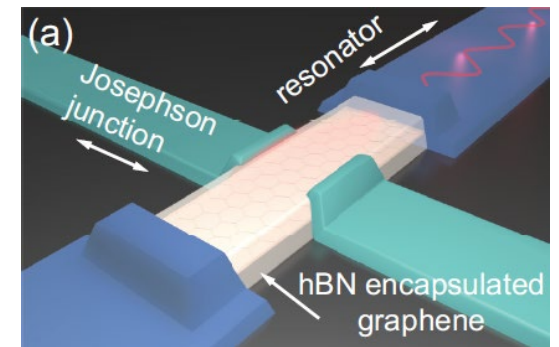


1,550-nm IR SPD



[Science 372, 409-412 (2021)]

Fundamentally limited
 Microwave bolometer



[Nature 586, 42-46 (2020)]

Summary

To be updated